Climatology and Trends Of Surface UV Radiation

SURVEY ARTICLE

D.W. Tarasick, V.E. Fioletov, D.I. Wardle, J.B. Kerr, L.J.B. McArthur and C.A. McLinden

Abstract *An improved understanding of the global UV climate has recently become of great interest. A number of stations are now making regular measurements of spectrally-resolved UV-B irradiance. Despite the lack of long-term records, it is possible to describe many of the short-term characteristics, dependencies and climatology of surface UV-B irradiance. This article describes the current state of UV-B measurements, and a climatology of surface UV-B irradiance with particular focus on Canada. The dependence of UV irradiance on ozone and other climate variables is discussed in detail, with reference to observations. In addition, comparison of radiative transfer models with recent measurements indicates that it is possible to infer surface UV-B irradiance from older records of total ozone and ancillary measurements (spectrally-integrated irradiance, aerosol optical depth and surface albedo) permitting the derivation of longer-term trends.*

Introduction

The ultraviolet solar spectrum is by common convention divided into three regions. Solar radiation of less than 280 nm wavelength (the UV-C region) is so strongly absorbed by ozone and (at shorter wavelengths) molecular oxygen that it is undetectable at the earth's surface. Surface UV irradiance[†] therefore consists of the UV-A (315-400 nm) and the UV-B (280-315 nm). While the former comprises a much larger portion of the total solar energy (7% of the extraterrestrial solar constant versus 1.5% for the UV-B portion) it has much less capacity to affect biological systems because the individual photons themselves are less energetic.

Irradiance in the UV-B part of the spectrum, however, is an important environmental concern because this energetic radiation can be quite harmful to plants and animals, as well as to exposed materials, like plastics and paints (UNEP*,* 1998; Gallagher *et al.,* 1997; Andrady *et al.,* 1995). In addition to the relatively well known health effects (cataracts, immunosuppression, and skin cancer) on human beings (Bergmanson *et al.,* 1996; Cullen and Perera, 1994; Gallagher *et al.,* 1995a,b; Garssen *et al.,* 1996), increases in surface UV-B irradiance (resulting from the well-known decline in total column ozone) may have deleterious effects on a great variety of species, such as the phytoplankton in the oceans that are the base of the marine food web (Cullen and Neale, 1994), nitrogen-fixing bacteria in rice paddies (Banerjee and Häder, 1996), food crops (Krupa and Kickert, 1989; Wilson and Greenberg, 1993a,b), forests (Laakso and Huttunen, 1998) and aquatic ecosystems (Pienitz and Vincent, 2000; Clair *et al.,* 2001). Several of these are particular concerns at mid-latitudes, including Canada. While some of these effects may be strictly proportional to cumulative UV-B dose, others may relate to the frequency of extreme UV-B events or to UV-B dose at particular times of the year, such as the early spring.

For these reasons an improved understanding of the global UV climate, including variability and trends in surface UV-B irradiance, has recently become of great interest. In this paper we review the current state of measurements and modeling of surface UV-B , discuss the climate variables that control surface UV-B irradiance, and present a brief climatology of surface UV-B irradiance based primarily on surface measurements at Canadian sites. Trends for Canadian latitudes from surface measurements and from satellite observations are also presented.

UV-B Measurements

Figure 1 shows the distribution of stations currently making regular measurements of UV-B radiation and submitting them to the World Ozone and UV-B Data Centre (WOUDC) in Toronto. A number of other sites, not indicated in Figure 1, also make regular measurements but do not report to the WOUDC. These stations are primarily in Europe and Australia. Approximately 60 stations are indicated in Figure 1. It will be apparent that the distribution of these sites is far from global: in fact most are located in North America.

The very large range of intensities over the spectrum of surface UV-B irradiance (see Figure 2) makes accurate UV-B measurements difficult, and it is only since the late 1980s that instruments

[†] Incident energy per unit area per unit time, from all directions (units W m^{-2}), as opposed to radiance, which is incident energy per unit solid angle per unit area per unit time (units W sr^{-1} m^{-2}). Spectral irradiance is incident energy per unit area per unit time per wavelength interval (units W m^{-2} nm^{-1}).

have been developed to make routine spectrally-resolved measurements of UV-B irradiance with the necessary accuracy and long-term stability. For this reason few spectral-measurement sites have been operating for more than 10 years. Most spectroradiometers that are used for UV monitoring have resolution in the range 0.3-1 nm, and take typically several minutes to complete a wavelength scan. All Canadian sites employ Brewer instruments, as do many other sites internationally. Several other types are also in use. Some 28 stations submit spectrally-resolved UV-B radiation data regularly to the WOUDC.

There are also several hundred broadband UV-B filter radiometers around the world, some of which have been operating for several decades. They also have the advantage of rapid response to changing conditions (i.e. clouds). Usually the filter transmission or the detector response characteristics are tailored to match a particular action spectrum, typically the erythemal spectrum. Unfortunately these instruments have proven to have insufficient stability in sensitivity and/or spectral response to reliably detect long-term trends (Deluisi and Barnett, 1992; Weatherhead *et al.,* 1997).

Multichannel filter instruments, employing several interference filters of moderate bandwidth, provide a compromise between single-channel broadband instruments and spectrometers. They can give accurate measurements of both total ozone and cloud optical depth as well as reasonable estimates of biologically effective UV irradiance (Dahlback, 1996), and are generally easier to characterise and calibrate than broadband UV radiometers (Slusser *et al.,* 1999; Gao *et al.,* 2002). Some 33 stations submit multi-filter radiometer data regularly to the WOUDC.

An interesting recent development is that of biological UV dosimeters: instruments that directly quantify the biologically effective solar irradiance for certain processes by using biological systems as UV sensors. A number of different sensors have been developed, based on direct DNA damage, the inactivation of bacterial spores and of bacteriophages, on photochemical reactions involving Vitamin D photosynthesis, and on polycrystalline uracil. Fairly good agreement with weighted spectrophotometric measurements has been shown for some systems (Furusawa *et al.,* 1998; Munakata *et al.,* 2000; Bérces *et al.,* 1999).

Measurements of total ozone from the Total Ozone Mapping Spectrometer (TOMS) and UV-A reflectivity at 380 nm (Herman *et al.,* 1996; 1999) as well as backscattered and reflected radiation at several wavelengths from the Earth Radiation Budget Experiment (ERBE) (Lubin *et al.,* 1998) have also been used to infer surface UV-B irradiance. Use of these satellite data sources permits UV-B irradiances to be estimated where they are not available by direct measurement (as is the case for much of the globe), and as far back as 1979. Similarly, total ozone measurements from The Global Ozone Monitoring Experiment (GOME) have been used along with Meteosat and ground-based data to infer surface UV-B irradiance at high (0.05º or 6 km^2) spatial resolution (Verdebout, 2000).

Surface UV-B irradiance has also been inferred from long-term records of total ozone and broadband solar radiation measured by pyranometers (McArthur *et al.,* 1999; Fioletov *et al.,* 2000; 2001; 2002; Gantner *et al.,* 2000). As for satellite measurements, these methods are indirect and necessarily involve some assumptions about the spectral characteristics of cloud and aerosol attenuation and surface reflectivity and hence are less accurate than direct measurements; however they offer an important opportunity to extend UV-B irradiance records back to the 1970s and 1960s.

Dependence of UV Irradiance on Ozone and other Climate Variables

Data from several spaceborne solar spectroradiometers have demonstrated that outside the Earth's atmosphere, solar UV radiation is remarkably constant with time, varying by less than 1%, mostly associated with the 27-day solar rotation period and the 11-year solar cycle (WMO, 1999; Lean *et al.,* 1997). The degree of variation is larger at shorter wavelengths: Lean *et al.* estimate 1.1% for the 200-300 nm band (averaged over the band) but only 0.25% for the 300-400 nm band, while the solar output averaged over all wavelengths varies by only 0.1%. Surface irradiance is affected, however, by many factors: solar zenith angle[†], absorption by ozone and other minor atmospheric constituents, scattering by clouds, scattering and absorption by atmospheric aerosols, scattering by air molecules (Rayleigh scattering) and surface albedo[‡].

Ozone is by far the most important absorber of UV radiation, as numerous observational studies have demonstrated (e.g., Kerr and McElroy, 1993; McKenzie *et al.,* 1999; Zerefos, 2002). Figure 2 illustrates this fact: comparing the extraterrestrial irradiance (A) with that calculated assuming only ozone absorption (D) and the clear-sky measured spectra (B) and (C), it is apparent that ozone absorbs 99% of the UV radiation at 298 nm, and 99.99% at 292 nm. Also apparent from this comparison is that Rayleigh scattering and aerosol scattering or absorption are responsible for an attenuation of about 40% that (compared to ozone absorption) is relatively independent of wavelength. No spectrally-dependent attenuation other than that due to ozone is evident; in fact although several atmospheric gases, including SO_2, NO_2, HNO_3 and CH_2O absorb in this spectral region, only SO_2 in occasional plumes from volcanoes or smokestacks is present in sufficient quantities to be unambiguously detected by UV spectroradiometers (WMO, 1999; Fioletov *et al.,* 1998; Krueger *et al.,* 1995; De Backer *et al.,* 1991). Changes in local SO_2 pollution have, however, been inferred from UV measurement time series (Zerefos, 2002).

Figure 2 (Curve E) also shows the erythemal action spectrum of the Commission internationale de l'éclairage (CIE). This spectrum is intended to approximately represent the wavelength-dependent effect of UV-B on human skin: specifically, for reddening of Caucasian skin (McKinlay and Diffey, 1987). Other action spectra exist, but this is the best known, and is the basis for the widely used UV Index (Kerr *et al.,* 1994; Burrows *et al.,* 1994). The UV Index is the integral of the UV irradiance weighted by the CIE erythemal action spectrum. It provides a convenient way of expressing changes in UV irradiance by a single (scalar) number.[§] It should be used with some caution, however, as it assumes not only the CIE spectral response for UV-B effects, but also that effects at different wavelengths are additive, and depend on dose (irradiation) rather than dose rate (irradiance). In general, the CIE-weighted irradiance increases by approximately 1.2% for a decrease of 1.0% in the ozone value. The ratio 1.2 is called the radiation amplification factor (RAF) of the CIE spectrum. Action spectra for plant damage (Quaite *et al.* 1992) and induction of squamous cell skin cancer in mice (deGruijl and van der Leun 1994) have RAFs that are also close to 1.2, while Setlow (1974) and Caldwell *et al.,* (1986) report RAFs close to 2, for DNA damage and UV damage to plants respectively. Madronich

[†] The angle between the sun and the zenith (vertical). The path length through the atmosphere is approximately proportional to the reciprocal of the cosine of the solar zenith angle.

[‡] The reflectance of the surface to UV radiation.

[§] Equal to the integrated UV-B irradiance in mW m^{-2}, divided by 25 mW m^{-2}.

(1992) finds RAFs ranging from 0.7 to 4.0, for several different action spectra, with latitude dependencies that are caused by nonlinearities in atmospheric absorption and scattering.

The remarkable attenuation by ozone of UV-B radiation is its most well-known feature. Figure 3 shows UV spectra recorded at Toronto on June 21, 1999, between about one-half hour after sunrise and local noon, corresponding to solar zenith angles between 85° and 20°. This figure also illustrates the fact that solar zenith angle is actually the most important factor in determining ground-level UV-B irradiance, since it determines the path length through the atmospheric ozone and other absorbers and scatterers (the airmass factor), and it varies during the day and throughout the year much more than any atmospheric constituent. As solar zenith angle increases, the irradiance at 325 nm is decreased by a factor of 50, while that at 300 nm decreases by a factor of 3000. This is further illustrated in Figure 4, showing model calculations for the effect of a 1% change in total ozone column on surface irradiance at different wavelengths, for a range of solar zenith angles. At the shorter wavelengths the Umkehr effect (Götz, 1931) may be seen: the change in UV irradiance increases with solar zenith angle up to a certain angle and then decreases. This is because when the direct path for solar irradiance becomes very long, absorption at short wavelengths becomes so great that the majority of photons detected at the surface are those that have been scattered in the middle atmosphere and therefore reach the ground via the relatively short vertical path through the ozone layer.

The dependence of the absorption path length on solar zenith angle implies that average UV-B irradiance is much less at mid-latitude and polar sites than in tropical regions, while the seasonal variation is much larger. The seasonal variation of the distribution of total ozone[†] with latitude reinforces this; the result is that the variation of UV-B irradiance with latitude is much greater in winter than in summer.

Next to ozone, cloud cover is the most important factor in reducing UV-B irradiance at the surface. In general, clouds act to reduce UV-B radiation more or less uniformly across the spectrum, as Figure 5 shows. This is because cloud droplet sizes are large with respect to UV and visible wavelengths. The overall effect of clouds is to reduce UV-B somewhat less than total irradiance, as the portion of the light that is reflected from the cloud layer and subsequently Rayleigh-scattered back by the atmosphere above the cloud to the ground is greater in the UV-B range than in the visible (Josefsson and Landelius, 2000; Kylling *et al.,* 1997). More importantly, where cloud cover is very heavy (Figure 5e, 5f) increased attenuation at shorter wavelengths is observed, presumably because multiple scattering increases path lengths through the clouds sufficiently that absorption by ozone and/or absorbing aerosols in the cloud deck becomes important (Mayer *et al.,* 1998).

Under overcast conditions attenuation can be as great as 99%, while summer haze has been observed to reduce UV-B in the range 5-23% (Estupiñán *et al.,* 1996). While uniform cloud and haze attenuate UV-B, increases of UV-B are observed under conditions of broken cloud, which can scatter or reflect radiation such that the total irradiance on the ground is not uniform, and at a particular location may be enhanced over that for clear-sky conditions (Mims and Frederick,

[†] The general circulation of the stratosphere, known as the Brewer-Dobson circulation, moves ozone from its primary source region above 30 km altitude in the tropics, toward mid-latitudes and the poles. This circulation is both strongest and most variable in winter, and so the highest ozone amounts and the most variability are found in winter at mid and higher latitudes.

1994). Intermittent enhancements of as much as 11% (Schafer *et al.,* 1996) and 27% (Estupiñán *et al.,* 1996) have been observed.

As may be expected, UV irradiance increases with altitude. In general the increase is significantly greater than would be expected from the reduction in the amount of ozone overhead. This is because of reduced scattering and aerosol absorption, as well as, frequently, the addition of snow cover. The decrease in Rayleigh attenuation[†] with altitude causes the direct flux to increase while the diffuse flux decreases; the total flux also increases (Krotov *et al.,* 1998). However, the variation of UV irradiance with altitude is complex, owing to the variability of aerosols and other scatterers and of ozone and other absorbers in the lower atmosphere, and it is not possible to characterize the change with altitude by a single number. For example, Seckmeyer *et al.* (1997) found that the monthly average erythemal irradiance was between 25% and 90% higher on the Zugspitze (3 km altitude) than at Garmisch-Partenkirchen (730 m altitude, 8 km distant). A comparison of seven spectrophotometers located in this same Alpine area showed increases in UV irradiance per 1000m altitude of 9% at 400 nm, 20% at 320 nm, and 30% at 300 nm, for low-aerosol conditions (Gröbner *et al.,* 2000). Observations at Mauna Loa (3.4 km latitude) indicate that the erythemal irradiance is 15-20% higher than at clean air sites near sea level. For overhead sun conditions, the largest value of erythemal irradiance was 0.51 Wm^{-2} (a UV Index of 20.4), which is probably the highest recorded value anywhere on the Earth's surface to date (Bodhaine *et al.,* 1996; 1997).

The effect of aerosols on UV-B irradiance is complex, owing to the variety of composition of aerosol material that may be present in the atmosphere, as well as its varying distribution. In general, the scattering from volcanic aerosol reduces the erythemal UV irradiance by about 5% (Tsitas and Yung, 1996). The largest reductions in UV are associated with dust and smoke plumes in Africa and South America. The observed reductions frequently exceed 50% (Herman *et al.,* 1999). The amount of UV irradiance reduction depends on the absorption properties of the aerosols. Most of the aerosols over North America are sulfates or other industrial pollutants which absorb UV only weakly and so reduce surface irradiance only by scattering, generally by about 10-20% (Krotov *et al.,* 1998). However, aerosol-induced reductions of UV-B by more than 50% have been observed in North America (McArthur *et al.,* 1999).

Surface UV-B irradiance also depends upon ground albedo, since some of the radiation reflected by the ground will be reflected back by the atmosphere. The atmosphere (diffusely) reflects radiation because of scattering by air molecules, aerosols and cloud droplets. The presence of snow has by far the largest effect, since the reflectivity of snow-free surfaces is small (typically between 0.02 and 0.08) while snow and ice-covered surfaces have reflectivities between 0.2 and more than 0.95 (Blumthaler and Ambach, 1988; Feister and Grewe, 1995). The highest values of UV albedo (0.96-0.98) have been measured for Antarctic snow, and were spectrally flat between 300 and 400 nm (Grenfell *et al.,* 1994). The overall effect is, however, wavelength dependent, in part because the downwelling irradiance is affected by the albedo of a large area around the point of measurement, and this is generally inhomogeneous (Webb *et al.,* 2000; Kylling *et al.,* 2000),

[†] The elastic scattering of photons by air molecules. As the number of scatterers in the path increases, with increasing depth of atmosphere, the direct flux is reduced, the scattered (diffuse) flux increases, and the total flux is reduced since the probability that a photon will be scattered back to space increases. At sea level for an overhead sun Rayleigh scattering reduces the direct flux at 313 nm by about e^{-1}. About half of the scattered flux reaches the surface as diffuse radiation.

and also because of the wavelength dependence of Rayleigh scattering and of ozone absorption of the reflected/scattered photons. Radiative transfer models indicate that the fraction of radiation reflected from the atmosphere back to the surface is about 0.4 for clear sky and 0.6 for cloudy conditions (Lenoble, 1998). This results in enhancements of surface UV-B irradiance for Arctic sites of 35-39% (Resolute, Churchill), while for urban sites enhancements vary between 8% (Halifax) and 22% (Montreal).

Solar UV irradiance is usually measured on a horizontal surface. In many real situations the irradiance incident on inclined surfaces is important: e.g., the human body, plant or building surfaces, atmospheric molecules in photochemical reactions. The importance of atmospherically scattered radiation (i.e., the diffuse component) in the UV means that exposures, and even the time of day of peak exposure, vary with both surface orientation and wavelength (Webb *et al.,* 1999; Grant and Heissler, 2000). Calculations and measurements of actinic fluxes (the radiation received by a spherical surface) show that using horizontal surface irradiances as a proxy can lead to significant errors (Kazadzis *et al.,* 2000; Hofzumahaus *et al.,* 1999).

An additional effect that is noticeable when comparing northern and southern hemisphere observations is the variation in earth-sun distance: the fact that the earth is somewhat farther from the sun in July than it is in January results in about 7% less solar radiation in the northern hemisphere summer than in the southern hemisphere summer.

Models

The physics of the processes affecting surface UV-B irradiance, viz. the absorption and scattering of radiation by the different constituents of the atmosphere and at the surface, is well understood, and it is possible to calculate surface irradiance quite accurately if accurate knowledge of the required input parameters is available. A variety of atmospheric radiative transfer models have been developed to calculate surface UV-B irradiance and/or actinic fluxes (e.g., Mayer *et al.,* 1997; Kylling *et al.,* 1998; Key, 1999; Madronich and Flocke, 1997; Ricchiazzi *et al.,* 1998; Ruggaber *et al.,* 1993; 1994; Davies *et al.,* 2000; Binyamin, 2002). A number of these codes have been published and made freely available. They require input parameters such as ozone, cloud conditions, aerosols, surface albedo, etc. that are measured or estimated. Such models typically solve the radiative transfer equation in a one-dimensional, plane-parallel atmosphere where atmospheric quantities (e.g., temperature, density, absorbers) are allowed to vary only in the vertical direction. A variety of numerical techniques are available to solve the radiative transfer equation (e.g., Hansen and Travis, 1974) and its solution yields the diffuse, or scattered, radiance as a function of altitude (or some other vertical co-ordinate) and direction. Direction is usually described in terms of a zenith angle, and for those models that resolve the azimuthal dependence, an azimuthal angle.

Once the diffuse UV-B radiances are known, surface irradiance is calculated by first integrating the downwelling surface radiance over solid angle. The direct component is also included, allowing for atmospheric attenuation of the extra-terrestrial solar flux, by $e^{-\tau(\lambda)\sec\vartheta}$, where τ is the vertically integrated optical depth, and ϑ is the solar zenith angle. Once the total (direct + diffuse) surface irradiance is known, integration over wavelength must be performed. A general spectral weighting term, $w(\lambda)$, is included and may represent, for example, an erythemal action spectrum (cf. Figure 2) or a filter response. If a spectrally narrow quantity is being computed, it

could represent an instrument function. For solar zenith angles larger than about 70º the sphericity of the Earth becomes important and the sec θ enhancement factor is no longer a good approximation. Instead, attenuation of the direct solar beam must be calculated using a Chapman function (e.g., Smith and Smith, 1972) or computed through a series of spherical shells.

The spectral quantities that are necessary to calculate UV-B irradiances (e.g., ozone absorption cross-sections, extra-terrestrial solar flux, Rayleigh cross-sections) are well known. It is generally the level of knowledge of atmospheric constituents which determines the accuracy of UV-B calculations.

For clear-sky conditions, with measured values of total ozone and aerosol optical depth, model calculations of spectrally integrated UV-B irradiance agree with measurements typically to within about 5% (Mayer *et al.,* 1997; Schwander *et al.,* 1997). If only the total ozone, but not the aerosol optical depth, is measured directly, errors of the order of 10-15% are likely. Optical depth information can sometimes be derived from the spectrally-resolved raw data used to derive the total ozone measurement (Marenco *et al.,* 2002). Measurements of other parameters, such as SO_2 content, ozone vertical distribution and ground albedo generally have a much smaller impact on the uncertainty in the integrated irradiance, although they may have more significant impact at certain wavelengths. An evident exception to this is (lack of) knowledge of whether the ground is snow-covered or not, as the drastic difference in surface albedo implied can lead to differences in integrated irradiance of more than 30%. Models have also been employed to tackle the more difficult problem of calculating surface UV-B irradiance in the presence of clouds: these calculations compare reasonably well with spectral irradiances measured under uniform cloud conditions or averaged over a large part of the sky, where some measurement of cloud attenuation is also available (WMO, 1999). Broken and inhomogeneous cloud fields present larger problems as the assumption of horizontal homogeneity in the plane-parallel solution breaks down. These situations require the use of computationally intensive, multi-dimensional models although there is an effort underway to relate a complex cloud field to a plane-parallel equivalent in terms of fraction of cloud cover and other parameters (Welsh and Wielicki, 1989; Weihs *et al.,* 2000).

Even though the error in (clear-sky) modeled total integrated irradiance is small, errors at particular wavelengths can be larger, especially at short wavelengths. Uncertainty in the total ozone measurement carries the largest potential for this kind of error, with errors of up to 17% at 300 nm and 50% at 290 nm for a 2.5% error in total ozone (Schwander *et al.,* 1997). Lack of knowledge of the vertical distribution of ozone introduces significant uncertainty at short wavelengths and large solar zenith angles, due to the Umkehr effect. Uncertainty in the tropospheric ozone amount and its distribution introduces smaller, but still significant potential error, as the greater incidence of multiple scattering in the troposphere increases the effective path length and so causes ozone there to be more effective at absorbing UV-B than the same amount of ozone in the stratosphere, except at lower solar elevations (Krotov *et al.,* 1998).

As an alternative to radiative transfer modeling, empirical, or statistical models have been widely used to establish an empirical relationship between different characteristics of UV-B irradiance and total ozone and other geophysical parameters. The predominant dependence in the absence of clouds, that on total ozone and the solar zenith angle, can be derived from a set of parallel measurements. This approach is used to estimate clear sky UV Index from the measured or

forecast total ozone, the solar zenith angle and/or day of the year (*e.g.* Burrows *et al.,* 1994; Austin *et al.,* 1994; Dubrovský 2000).

Under cloudy conditions, UV irradiance can be derived from the ozone amount and some parameter of cloud cover. That parameter can be derived from a different wavelength region or a different viewing geometry. Thus meteorological cloudiness data can be used with ozone to generate UV irradiance (Bais *et al*., 1993), as can global solar radiation in the range 300-3000 nm, measured by pyranometers. Analysis of parallel measurements at different sites has demonstrated that different characteristics of UV irradiance could be derived from global solar radiation data and ozone (Ito *et al.*, 1993; Frederick *et al.,* 1993; Bordewijk *et al.,* 1995; Bodeker and McKenzie, 1996). These studies found that the UV reduction factor, *i.e.* the ratio of UV irradiance to its clear sky value, could be represented by a nonlinear function of the global radiation reduction factor and the solar zenith angle. Several studies (*e.g.* Foyo-Moreno *et al.,* 1999; den Outer *et al.,* 2000; Matthijsen *et al.,* 2000; McArthur *et al.,* 1999; Fioletov *et al.,* 2001) have suggested empirical parameterizations to derive spectrally integrated characteristics of UV irradiance from pyranometer measurements.

UV-B Climatology

A number of sites, many of them in Canada, now have long enough records of continuous observation to make it possible to describe the short-term characteristics and climatology of surface UV-B irradiance. Figure 6 shows daily observations for a number of Canadian and other sites, summarized as UV Index values (the original data, available from the WOUDC, are full spectral scans, from 290 to 325 nm at 0.5 nm resolution). For each day, the maximum value observed is shown. Also shown is an estimate of the average daily maximum clear-sky UV Index at each site for the pre-1980 period, that is, previous to significant ozone decline. This estimate is based on observed pre-1980 ozone values, where available, with appropriate adjustment where these records are sparse (as in the case of Alert) or from TOMS ozone data, adjusted by comparison with the stations with long records (as in the case of San Diego). The calculation of UV Index from the ozone data is via an empirical relationship based on UV-B and ozone values observed at Toronto for snow-free conditions (see Beattie *et al.,* 1995 for a description). It includes adjustment for variations in the earth-to-sun distance, and so works reasonably well even for Syowa, Antarctica. However, it clearly underestimates historical UV-B for Mauna Loa, as it is based on Toronto data, and hence on near sea-level values for the ozone vertical distribution. It is also not entirely accurate at low sun angles, as shown by the spurious increases, for example, at Edmonton and Goose Bay in December. Other departures from this curve are enhancements due to ozone depletion since 1980 and to snow cover. Also superimposed on each plot are the most recent complete year of observations for each site, in order to show the day-to-day variability.

The most evident feature of all these figures is the high degree of variability; this is primarily due to clouds and so is more pronounced at cloudy sites, such as Halifax and Goose Bay, and much less so at Mauna Loa. Smaller variations, which can be positive as well as negative, are due to ozone variability. Also apparent, at most of the Canadian sites as well as San Diego, is that maximum clear-sky UV Index values in the 1990s were higher than those calculated for the pre-1980 period, by about 10%, which is what would be expected, based on an average total ozone decline of about 6-7% over this period and an RAF of 1.2. As well, dramatically higher UV

Index values are seen at Syowa during the antarctic spring, due, of course, to the appearance of the ozone hole (which first became evident in about 1984). Peak values are similar to those in June at San Diego.

For the mid-latitude sites, the pre-1980 climatology indicates higher UV levels at the fall equinox than the spring equinox, as ozone levels are typically 30% lower in fall than spring. However, at many of the Canadian sites, particularly Resolute, Churchill, Alert, Edmonton, Saskatoon and Winnipeg, but also at Montreal, Goose Bay and Toronto, observed UV-B values in spring typically exceed the climatology by much more than 10%. These enhancements are due to snow (which was not included in the climatology).

An estimated surface UV-B irradiance climatology for all of Canada has been developed recently from long-term records of broadband solar radiation measured by pyranometers at 45 sites, as well as total ozone, snow cover and dew point data (Fioletov *et al.,* 2002).

Trends in Surface UV-B Irradiance

The quantification of long-term changes in the amount of UV-B radiation reaching the earth's surface is more difficult than the corresponding problem of detecting changes in average ozone levels. Ozone has been studied, and regularly measured, since the 1920s. In Canada a continuous record of daily measurements exists at some sites since the 1950s. Worldwide, a large data base of ozone measurements exists for the 1950s and 1960s, long before ozone depletion became a scientific issue, because at this time it was thought that research into stratospheric motion, of which ozone is a useful tracer, would lead to improved models for forecasting the weather. In contrast, it is only since the late 1980s that instruments have been developed and deployed to make routine spectrally-resolved measurements of UV-B irradiance, suitable for the determination of trends. This is due in part to the difficulty of making absolute intensity measurements (in contrast to the relative intensity measurements from which ozone is derived); careful and frequent attention must be paid to maintaining calibration integrity and traceability (Webb *et al.,* 1998). In addition, the confounding influences of changes in cloud cover, aerosols, and surface albedo increase the variability in the time series and hence the difficulty of detecting trends (Weatherhead *et al.,* 1998).

From the discussion in the preceding sections, however, one would expect that changes in UV-B irradiance could simply be calculated from the measured changes in total ozone. Unfortunately, the earliest study on surface UV-B trends, employing data from a network of broad-band filter (Robertson-Berger) meters, found *negative* trends over the United States from 1974-1985 (Scotto *et al.,* 1988), a time when ozone levels were known to be decreasing. This implied that a positive trend in aerosols or cloudiness was overwhelming the effect of decreasing ozone. It was later shown that calibration changes or other instrument-related problems were responsible for the negative trend (Deluisi and Barnett, 1992; Weatherhead *et al.,* 1997). Subsequently Kerr and McElroy (1993) found a positive trend in spectral UV data taken at Toronto between 1989 and 1993, of similar magnitude to the ozone decrease over the period, thereby demonstrating that year-to-year cloud variability did not overwhelm the ozone-induced trend in total irradiation. Herman *et al.* (1996) have inferred significant trends in zonally averaged surface UV-B irradiance over the entire globe poleward of 45°, using TOMS measurements of total ozone and UV-A reflectivity at 380 nm. The TOMS data also showed no changes in zonally averaged

aerosol and cloud reflectivity, indicating that the trends were real and due to ozone decreases. More recently, McKenzie *et al.* (1999) have shown that peak summertime UV-B values at Lauder, N.Z. have increased by about 12% in response to ozone decreases over the period 1990-1999.

Figure 7 shows trends in zonally-averaged erythemal UV-B for the period 1979-1999. This is an update of the similar figure in Herman *et al.,* (1996), and includes the effects of clouds. Data from Nimbus-7 TOMS (1979-1993) and EarthProbe TOMS (1996-1999) have been combined in this analysis. No correction for bias was required, as both instruments show stable in-flight calibration and compare extremely well with ground-based ozone time series (e.g. Herman *et al.* 1999). The TOMS erythemal UV-B data product is derived (Herman *et al.* 1996; 1999) by first computing the clear-sky UV-B irradiance, using the same table of solutions of the radiative transfer equation as in the TOMS ozone retrievals. A climatological database is used to determine the probability of presence of snow/ice in the instrument's field of view, in which case a surface albedo of 40% is assumed. The 380 nm (Nimbus-7) or 360 nm (EarthProbe) radiances, solar and viewing angles, terrain height, and assumed surface albedos are used to derive an estimate of cloud/aerosol optical thickness, using tables of solutions of the radiative transfer equation at these wavelengths. The attenuation of the global irradiance due to a model uniform cloud of that optical thickness is then computed. The precision of surface UV-B irradiance values estimated in this manner from TOMS is believed to be ± 6%, although a detailed comparison with Brewer measurements at Toronto suggests that the TOMS irradiances are systematically about 15% too high (Herman *et al.,* 1999). Recent improvements to the algorithm include correction for the effects of UV-absorbing aerosols, and better cloud and ground albedo (snow) corrections (Taalas *et al.,* 2002).

Figure 8 shows the TOMS erythemal-action-spectrum-weighted UV time series, including cloud effects, for Canadian latitudes, estimated from TOMS (1979-1999) data, for summer (May-August) and winter (November-February) months. These are presented as seasonal averages of monthly means. Like the previous figure, it shows significant trends in UV-B over the 20-year period that includes the large ozone decline of the 1980s and early 1990s. Winter trends are about twice as large as summer trends, primarily because of the larger degree of winter ozone loss, although changes in snow cover may also have had an effect (see below). The effects of the large springtime ozone losses of 1993 and in the Arctic in 1997 are clearly evident.

Unfortunately ground-based UV spectral instruments have not yet been able to detect significant trends in average irradiation. This is primarily due to the short time series of measurements to date: very few stations have even the eleven years of data needed to cover a solar cycle. In addition, observations from a single site experience much more variability due to local variations in cloud and snow than do satellite measurements, which average over larger areas. Figure 9 shows the time series of observations from Toronto and Saskatoon, two sites with the longest records of spectrally-resolved measurements of UV-B irradiance currently available (11 years). These are presented as seasonal averages of monthly means. Trends (indicated by the linear regression fits) are all non-significant. In large part this is due to the fact that total ozone has not changed as much over this period as over the previous decade; the trend in total ozone at Toronto for the 1989-2000 period is only –0.55 ± 2.56% per decade.

This implies that it is of particular interest to attempt to describe changes in surface UV-B irradiance since before the recent decline in mid-latitude total ozone; that is, since before about 1980. This has been recently done for three Canadian sites, using long-term records of total ozone and broadband solar radiation measured by pyranometers, as well as observations of local snow cover (Fioletov *et al.,* 2000; 2001). These results are reproduced in Table 1. All three sites show statistically significant increases over the period 1979-1997. The effect of snow and cloud cover on the trends at Churchill is particularly interesting: while the clear-sky, snow-free trend is of similar magnitude but opposite sign to the total ozone trend, apparent trends in snow and cloud cover at this site increase this trend by about 50% and 100% respectively, for an overall increase in surface UV-B irradiance that is 2.5 times greater than the corresponding clear-sky, snow-free trend.

Table 1: Trends in total ozone and derived CIE UV radiation in % per decade. Errors are 2σ confidence intervals. UV irradiance is derived from total ozone, broadband (pyranometer) measurements, and observations of local snow cover. Data are for the period 1979-1997. The term "Cloud free" denotes that calculations were performed assuming clear skies at all times, while "Snow free" means that calculations neglected any enhancement of UV due to ground albedo. "All terms" means that the terms in the statistical model representing cloud and snow effects were included, using actual data.

Station	Nov-Feb		Mar-Apr		May-Aug		Sep-Oct		Year	
					Total Ozone					
Churchill	-4.0	±2.9	-3.9	±2.9	-4.3	±1.6	-1.8	±2.4	-3.8	±1.4
Edmonton	-2.9	±2.6	-5.4	±2.9	-4.7	±1.7	-1.4	±2.8	-3.8	±1.4
Toronto	-3.0	±2.5	-5.4	±2.7	-3.4	±1.6	-1.8	±2.5	-3.4	±1.3
					Derived UV, Cloud free, Snow free					
Churchill	4.3	±3.0	5.0	±5.5	4.4	±1.8	5.9	±5.5	4.6	±1.7
Edmonton	2.2	±2.3	6.1	±3.0	5.4	±1.6	4.7	±3.9	5.3	±1.3
Toronto	2.7	±2.3	5.9	±3.0	3.3	±1.4	1.8	±2.4	3.4	±1.2
					Derived UV, Cloud free					
Churchill	4.6	±3.0	5.0	±5.4	6.3	±2.4	5.6	±5.0	6.0	±2.0
Edmonton	3.4	±3.3	5.4	±3.2	5.4	±1.8	4.6	±4.3	5.2	±1.5
Toronto	2.6	±2.3	6.6	±3.2	3.3	±1.3	1.8	±2.4	3.6	±1.2
					Derived UV, Snow free					
Churchill	9.6	±3.8	12.1	±6.6	9.1	±4.2	6.5	±6.9	9.3	±3.3
Edmonton	4.7	±4.6	3.8	±4.2	3.5	±3.8	4.9	±9.1	3.8	±2.9
Toronto	0.8	±5.1	3.5	±5.8	3.7	±3.5	2.9	±6.2	3.3	±2.6
					Derived UV, all terms					
Churchill	9.9	±4.0	12.2	±6.8	11.3	±5.1	6.2	±7.4	10.9	±3.9
Edmonton	5.6	±4.9	3.4	±4.7	3.5	±3.8	4.7	±9.2	3.8	±2.9
Toronto	0.8	±5.1	4.2	±5.7	3.7	±3.5	2.9	±6.2	3.4	±2.6

Gantner *et al.* (2000) have derived trends in UV-B from pyranometer data at Hohenpeissenberg, in southern Germany, for snow and cloud-free conditions over the period 1968-1997. They find trends similar to those above for the summer and fall, but 2-3 times larger in March and April.

Conclusion

The number of stations making regular spectrally-resolved measurements of UV-B is increasing rapidly, so that in another decade it may be possible to provide a fairly complete description of global surface UV irradiance, in much the same way as can be done for total ozone. While to some extent this can be done already from satellite measurements, this approach is limited by the fact that surface UV is strongly affected by local conditions, particularly clouds and snow. For this reason ground-based spectral UV-B measurements will continue to be required for detailed studies of UV-B effects. An increased interaction between the measurement community and those investigating effects may be especially fruitful in the future. Better knowledge of how effects on biological systems and on exposed materials relate to such parameters as cumulative UV-B dose, frequency of extreme UV-B events or to UV-B dose at particular times of the year may influence analyses of past and future changes, and trends in UV-B irradiance.

References

Andrady, A.L., M.B. Amin, S.H. Hamid, X. Hu, and A. Torikai, 1995. Effects of increased solar ultraviolet radiation on materials. *Ambio,* **24** (3), 191–196.

Austin J., B. R. Barwell, S. J. Cox, P. A. Hughes, J.R. Knight, G. Ross, P. Sinclair, and A. R. Webb, 1994: The diagnosis and forecast of clear sky ultraviolet at the Earth's surface. *Meteor. Apps.,* **1**, 321-336.

Bais A. F., S. Kazadzis, D. Balis, C. Zerefos, and M. Blumthaler, Correcting global solar ultraviolet spectra recorded by a Brewer spectroradiometer for its angular response error, *Appl. Opt.,* **37**, 6339-6344, 1998.

Bais, A. F., C. S. Zerefos, C. Meleti, I. C. Ziomas, and K. Tourpali, Spectral measurements of solar UVB radiation and its relations to total ozone, SO_2, and clouds, *J. Geophys. Res*., *98*, 5199-5204, 1993.

Banerjee, M. and Häder, D.-P. 1996. Effects of UV radiation on the rice field cyanobacterium, *Aulosira fertilissima*. *Environmental and Experimental Botany,* **36,** 281-291.

Beattie, B., K. Keddy, D. Tarasick and J. Kerr (1995) *Pre-1980 Ultraviolet Index Climatology for Canadian Locations,* Report MAES 1-95, Environment Canada, Atlantic Region.

Bérces A., S. Fekete, P. Gáspá, P. Gróf, P. Rettberg, G. Horneck and G. Rontó, UV dosimeters in the assessment of the biological hazard from environmental radiation, *J. Photochem. Photobiol.* B: Biol. **53**, 36-43, 1999.

Bergmanson, J., T. Sheldon, and A.P. Cullen, 1996. A sting in the rays. *Optician,* **212** (5560), 17–22.

Binyamin, J., 2002. Modelling UV-B irradiance for Canada. Ph.D. thesis, McMaster University, Canada.

Blumthaler, M. and W. Ambach (1988) Solar UVB-albedo of various surfaces. *Photochem. Photobiol.,* **48**, 85-88.

Bodeker, G. E. and R. L. McKenzie, 1996: An algorithm for inferring surface UV irradiance including cloud effects. *J. Appl., Meteor.,* **35**, 1860-1877.

Bodhaine, B.A., R.L. McKenzie, P.V. Johnston, D.J. Hofmann, E.G. Dutton, R.C. Schnell, J.E. Barnes, S.C. Ryan and M. Kotkamp (1996) New ultraviolet spectroradiometer measurements at Mauna Loa Observatory. *Geophys. Res. Lett.,* **23**, 2121–2124.

Bodhaine, B.A., E.G. Dutton, D.J. Hofmann, R.L. McKenzie and P.V. Johnston (1997) UV measurements at Mauna Loa: July 1995 to July 1996. *J. Geophys. Res.,* **102**, 19265-19273.

Bordewijk, J. A., H. Slaper, H. A. M. Reinen, and E. Schlamann, 1995: Total solar radiation and the influence of clouds and aerosol on the biologically effective UV. *Geophys. Res. Lett.,* **22**, 2151-2154.

Brueckner, G.E., K.L. Edlow, L.E. Floyd IV, J.L. Lean and M.E. VanHoosier, The Solar Ultraviolet Spectral Irradiance Monitor (SUSIM) experiment on board the Upper Atmosphere Research Satellite (UARS), *J. Geophys. Res.,* **98**, 10695-10711, 1993.

Burrows, W., M. Vallee, D.I. Wardle, J.B. Kerr, L.J. Wilson and D.W. Tarasick (1994) The Canadian UV-B and total ozone forecast model. *Met. Apps.,* **1**, 247–265.

Caldwell, M.M., L.B. Camp, C.W. Warner, and S.D. Flint (1986) Action spectra and their key role in assessing biological consequences of solar UV-B radiation change. In: Worrest, R.C. and M.M. Caldwell (eds.) *Stratospheric Ozone Reduction, Solar Ultraviolet Radiation, and Plant Life.* Springer-Verlag, Berlin, pp. 87–111

Clair, T. A., J. Ehrman, I. Kaczmarska, A. Locke, D.W. Tarasick, K.E. Day, and G. Maillet (2001) Will reduced summer UV-B levels affect summer zooplankton populations of temperate acid, humic and clearwater lakes?, *Hydrobiologia,* **462**, 75-89.

Cullen, A.P., and S.C. Perera, 1994. Sunlight and human conjunctival action spectrum. Ultraviolet radiation hazards. *SPIE Proceedings,* **2134**, 24–30.

Cullen, J.J., and P.J. Neale, 1994. Ultraviolet radiation, ozone depletion, and marine photosynthesis. *Photosyn. Res.,* **39**, 303–320.

Dahlback, A., 1996. Measurements of biologically effective UV doses, total ozone abundances, and cloud effects with multichannel, moderate bandwidth filter instruments. *Appl. Opt.* **35**, 6514-6521.

Davies, J., P. Kuhn, G. Duhamel, J. Binyamin and K. Runnalls, 2000. An ultraviolet (290 to 325 nm) irradiation model for southern Canadian conditions. *Physical Geography,* **21**, 4, 327-344.

De Backer, H., and D. De Muer, Intercomparison of total ozone data measured with Dobson and Brewer spectrophotometers at Uccle (Belgium) from January 1984 to March 1991, including zenith sky observations, *J. Geophys. Res.,* **96**, 20,711-20,719, 1991.

deGruijl, F.R., and J.C. van der Leun (1994) Estimate of the wavelength dependency of ultraviolet carcinogenesis in humans and its relevance to risk assessment of stratospheric ozone depletion. *Health Physics,* **67**, 319–325.

Deluisi, J.J. and J. Barnett (1992) An examination of the calibration stability of the US Robertson-Berger meter network (abstract). *EOS Trans. Amer. Geophys. Union,* **73**, (43), Fall Meeting Suppl., 110.

den Outer, P. N., H. Slaper, J. Mattijsen, H. A. J. M. Reinen, and R. Tax, 2000: Variability of ground-level ultraviolet: model and measurement. *Radiat. Protect. Dosimetry,* **91**, 105-110.

Dubrovský, M. Analysis of UV-B irradiances measured simultaneously at two stations in the Czech Republic. *J. Geophys. Res.,* **105**, 4907-4913, 2000.

Estupiñán, J.G., S. Raman, G.H. Crescenti, J.J. Streicher and W.F. Barnard (1996) Effects of clouds and haze on UV-B radiation. *J. Geophys. Res.,* **101**, 16807-16816.

Feister, U. and R. Grewe (1995) Spectral albedo measurements in the UV and visible region over different types of surfaces. *Photochem. Photobiol.,* **62**, 736-744.

Fioletov, V.E., and W.F.J. Evans, The influence of ozone and other factors on surface radiation, in *Ozone Science: A Canadian Perspective on the Changing Ozone Layer*, edited by D.I. Wardle, J.B. Kerr, C.T. McElroy and D.R. Francis, Environment Canada, University of Toronto Press, Toronto, 1997.

Fioletov, V.E., J.B. Kerr, and D.I. Wardle, The relationship between total ozone and spectral UV irradiance from Brewer observations and its use for derivation of total ozone from UV measurements, *Geophys. Res. Lett.,* 24, 2997-3000, 1997.

Fioletov, V.E., E. Griffioen, J.B. Kerr, D.I. Wardle and O. Uchino (1998) Influence of volcanic sulfur dioxide on spectral UV irradiance as measured by Brewer spectrophotometers. *Geophys. Res. Lett.,* **25**, 1665-1668.

Fioletov, V., B. McArthur, J. Kerr and D. Wardle (2000) Estimation of long-term changes in ultraviolet radiation over Canada. In: *Atmospheric Ozone, Proceedings of the Quadrennial Ozone Symposium, Sapporo 2000.* NASDA, Sapporo, pp. 231-232.

Fioletov, V.E., L.J.B. McArthur, J.B. Kerr and D.I. Wardle (2001) Long-term variations of UV-B irradiance over Canada estimated from Brewer observations and derived from ozone and pyranometer measurements. *J. Geophys. Res.,* **106**, 23009-23028.

Fioletov, V.E., L.J.B. McArthur, J.B Kerr and D.I. Wardle (2003) Estimating UV Index climatology over Canada. *J. Appl. Meteor.*, in press.

Foyo-Moreno I., J. Vida, and L. Alados-Arboledas, 1999: A Simple All Weather Model to Estimate Ultraviolet Solar Radiation (290–385 nm). *J. Appl. Meteor.,* **38**, 1020–1026.

Frederick J. E., A. E. Koob, A. D. Alberts, and E. C. Weatherhead, 1993: Empirical studies of tropospheric transmission in the ultraviolet: broadband measurements. *J. Appl. Meteor.,* **32**, 1883-1892.

Furusawa, Y., L.E. Quintern, H. Holtschmidt, P. Koepke and M. Saito, Determination of erythema-effective solar radiation in Japan an Germany with a spore monilayer film optimized for the detection of UVB and UVA - results of a field campaign. *Appl. Microbiol. Biotechnol,.* **50**, (1998) 597-603

Gallagher, R.P., G.B. Hill, C.D. Bajdik, S. Fincham, A.J. Coldman, and D.I. McLean, 1995a. Sunlight exposure, pigmentation factors, and risk of non-melanocytic skin cancer: I – basal cell carcinoma. *Arch. Dermatol.,* **131**, 157–163

Gallagher, R.P., G.B. Hill, C.D. Bajdik, S. Fincham, A.J. Coldman, and D.I. McLean (1995b). Sunlight exposure, pigmentation factors, and risk of non-melanocytic skin cancer: II – squamous cell carcinoma. *Arch. Dermatol.,* **131**, 164–169.

Gallagher, R.P., M. Morrison, K. Percy, H. Vaughn, J. Cullen and R. Alward (1997) UV-B Effects, in *Ozone Science: A Canadian Perspective on the Changing Ozone Layer*, edited by D.I. Wardle, J.B. Kerr, C.T. McElroy and D.R. Francis, Environment Canada, University of Toronto Press, Toronto, 1997.

Gantner, L., P. Winkler and U. Koehler, A method to derive long-term time series and trends of UV-B radiation (1968-1997) from observations at Hohenpeissenberg (Bavaria), *J. Geophys. Res.,* **105**, 4879-4888, 2000.

Gao, W., J.R. Slusser, L.C. Harrison, P. Disterhoft, Q. Min, B. Olsen, K, Lantz and B. Davis (2002) Comparisons of UV synthetic spectra retrieved from the USDA UV multi-filter rotating shadow-band radiometer with collocated USDA reference UV spectroradiometer and

NIWA UV spectroradiometer. In: *Ultraviolet Ground- and Space-based Measurements, Models and Effects,* J.R. Slusser, J.R. Herman, W. Gao, Editors, Proceedings of SPIE, Vol. 4482, pp. 408-414.

Garssen, J., W. Goettsch, F. de Gruize, W. Slob, and H. Van Loveren (1996). Risk assessment of UVB effects on resistance to infectious diseases. *Photochem. Photobiol.,* **64**, 269–294.

Götz, F. W. P. (1931) Zum Strahlungsklima des Spitzbergen-sommers. Strahlungs- und Ozonmessungen in der Königsbucht 1929. *Gerlands Beiträge zur Geophys.,* **31**, 119-154.

Grant, R.H., and G.M. Heisler (2000). Multi-waveband solar irradiance on tree-shaded vertical and horizontal surfaces: cloud-free and partly cloudy skies. *Photochem. Photobiol.,* **73**, 24-31.

Grenfell, T.C., S.G. Warren and P.C. Mullen (1994) Reflection of solar radiation by the Antarctic snow surface at ultraviolet, visible, and near-infrared wavelegths. *J. Geophys. Res.,* **99**, 18669-18684.

Gröbner J., A. Albold, M. Blumthaler, T. Cabot, A. De la Casinieri, J. Lenoble, T. Martin, D. Masserot, M. Müller, R. Philipona, T. Pichler, E. Pougatch, G. Rengarajan, D. Schmucki, G. Seckmeyer, C. Sergent, M. L. Touré and P. Weihs. (2000) Variability of spectral solar ultraviolet irradiance in an Alpine environment; *J. Geophys. Res.,* **105**, 26991-27003.

Hanson, J. E. and L. D. Travis (1974) Light scattering in planetary atmosphere, *Space Sci. Rev.*, **16**, 527-610.

Herman J. R., P.K. Bhartia, J. Ziemke Z. Ahmad and D. Larko (1996) UV-B increases (1979-1992) from decreases in total ozone. *Geophys. Res. Lett.,* **23**, 2117–2120.

Herman J. R., N. Krotov, E. Celarier, D. Larko and G. Labow (1999) Distribution of UV radiation at the Earth's surface from TOMS-measured UV-backscattered radiances. *J. Geophys. Res.,* **104**, 12059-12076.

Hofzumahaus, A., A. Kraus and M. Mueller, Solar actinic flux spectroradiometry: a technique for measuring photolysis frequencies in the atmosphere, *Appl. Opt.,* **38**, 4443-4460, 1999.

Ito, T., Y. Sakoda, T. Uekubo, H. Naganuma, M. Fukuda, and M.Hayashi, 1993: Scientific application of UV-B observations from JMA network. *Proc. 13th UOEH Int. Symp. And the Second Pan Pacific Cooperative Symp. On Impact of Increased UV-B exposure on Human Health and Ecosystem*, Kitakyushu, Japan, University of Occupational and Environmental Health, 107-125.

Josefsson W. and T. Landelius, Effect of clouds on UV irradiance: As estimated from cloud amount, cloud type, precipitation, global radiation and sunshine duration, *J. Geophys. Res.,* **105**, 4927-4935, 2000.

Kazadzis S., A.F. Bais, D. Balis, C.S. Zerefos and M. Blumthaler, Retrieval of downwelling UV actinic flux density spectra from spectral measurements of global and direct solar UV irradiance; *J. Geophys. Res.*, **105**, 4857-4864, 2000.

Kerr, J.B. and C.T. McElroy (1993) Evidence for large upward trends of ultraviolet-B radiation linked to ozone depletion. *Science*, **262**, 1032-1043.

Kerr J.B., C.T. McElroy, D.W. Tarasick and D.I. Wardle (1994) The Canadian Ozone Watch and UV-B advisory programs. In: *Ozone in the Troposphere and Stratosphere, Proceedings of the Quadrennial Ozone Symposium 1992.* NASA Conference Publication 3266, Springer-Verlag, Berlin, pp. 794–797.

Key J.R., *Streamer - User's Guide*, NOAA / NESDIS / ORA / ARAD / ASPT Cooperative Institute for Meteorological Satellite Studies, University of Wiconson, Madison, available at http://stratus.ssec.wisc.edu/streamer/streamer.html, 1999.

Krotov, N.A., P.K. Bhartia, J.R. Herman, V. Fioletov and J. Kerr (1998) Satellite estimation of spectral surface irradiance in the presence of tropospheric aerosols 1. Cloud-free case. *J. Geophys. Res.,* **103**, 8779-8793.

Krueger, A. J., L. S. Walter, P. K. Bhartia, C. C. Schnetzler, N. A. Krotkov, I. Sprod, and G. J. S. Bluth, Volcanic sulfur dioxide measurements from the total ozone mapping spectrometer instruments, *J. Geophys. Res.,* **100**, 14,057-14,076, 1995.

Krupa, S.V., and R.N. Kickert, 1989. The greenhouse effects: impact of UV-B, CO_2 , and O3 on vegetation. *Environmental Pollution,* **61**, 263–393.

Kylling A., A. Albold, and G. Seckmeyer, 1997. Transmittance of a cloud is wavelength-dependent in the UV-range: Physical interpretation. *Geophys. Res. Lett.,* **24**, 397-400.

Kylling, A., A.F. Bais, M. Blumthaler, J. Schreder, and C.S. Zerefos, Effect of aerosols on solar UV irradiances during the Photochemical Activity and Solar Ultraviolet Radiation campaign, *J. Geophys. Res.,* **103**, D20, 26,051-26,060, 1998.

Kylling A., T. Persen, B. Mayer and T. Svenoe, Determination of an Effective Spectral Surface Albedo From Ground Based Global and Direct UV Irradiance Measurements, *J. Geophys. Res.,* **105**, 4949-4959, 2000.

Laakso K. and S. Huttunen, Effects of ultraviolet-B radiation on conifers: a review, *Environmental Pollution,* **99**, 319-328, 1998.

Lean, J.L., G.L. Rottman, H.L. Kyle, T.N. Woods, J.R. Hickey and L.C. Puga (1997) Detection and parameterization of variations in solar mid- and near-ultraviolet radiation (200-400 nm). *J. Geophys. Res.,* **102**, 29939-29956.

Lenoble, J. (1998) Modeling of the influence of snow reflectance on ultraviolet radiance for cloudless sky. *Appl. Opt.,* **37**, 2441-2447.

Lubin, D., E.H. Jensen and H.P. Gies (1998) Global surface ultraviolet radiation climatology from TOMS and ERBE data. *J. Geophys. Res.,* **103**, 26061-26091.

Madronich, S. (1992) Implications of recent total ozone measurements for biologically active ultraviolet radiation reaching the Earth's surface. *Geophys. Res. Lett.,* **1**9, 37–40.

Madronich S. and S. Flocke, Solar Ultraviolet Radiation. Modelling, Measurements and Effects, in Theoretical estimation of biologically effective UV radiation at the Earth's surface, Springer-Verlag Berlin, Heidelberg, Eds. Zerefos. C.S. and A.F. Bais, NATO ASI, 1997

Marenco, F., A. di Sarra and J. De Luisi (2002) Methodology for determining aerosol optical depth from Brewer 300-320-nm ozone measurements. *Appl. Opt.,* **41**, 1805-1814.

Matthijsen, J., H. Slaper, H. A. J.M.Reinen, and G. J. M. Velders, 2000: Reduction of solar UV by clouds: Comparison between satellite-derived cloud effects and ground-based radiation measurements. *J. Geophys.Res*., **105**, 5069-5080.

Mayer, B., G. Seckmeyer, and A. Kylling, Systematic longterm comparison of spectral UV measurements and UVSPEC modeling results. *J. Geophys. Res.,* **102** (D7): 8755-8768, 1997

Mayer B., A. Kylling, S. Madronich, and G. Seckmeyer, Enhanced absorption of UV radiation due to multiple scattering in clouds: Experimental evidence and theoretical explanation, *J. Geophys. Res*., **103**, 31,241-31,254, 1998.

Mims, F. M., and J. E. Frederick, Cumulus clouds and UV-B, *Nature,* **371**, 291-291, 1994.

McArthur, L.J.B., V.E. Fioletov, J.B. Kerr, C.T. McElroy and D.I. Wardle (1999) Derivation of UV-A irradiance from pyranometer measurements. *J. Geophys. Res.,* **104**, 30139-30151.

McKenzie, R., B. Connor and G. Bodeker (1999) Increased summertime UV radiation in New Zealand in response to ozone loss. *Science*, **285**, 1709-1711.

McKinlay, A.F. and B.L. Diffey (1987) A reference action spectrum for ultraviolet induced erythema in human skin. In: Passchier, W.R. and B.M.F. Bosnajakovich (eds.) *Human Exposure to Ultraviolet Radiation: Risks and Regulations.* Elsevier, Amsterdam, pp. 83-87.

Molina, T.J. and M.J. Molina, Absolute absorption cross sections of ozone in the 185- to 350-nm wavelength range. *J. Geophys. Res.,* **91**, 14501-14508, 1986.

Munakata, N., S. Kazadzis, A. Bais, K. Hieda, G. Rontó, P. Rettberg and G. Horneck, Comparisons of Spore Dosimetry and Spectral Photometry of Solar-UV Radiation at Four Sites in Japan and Europe, *Photochem. Photobiol.* **72**, 739-745, 2000.

Pienitz R. and W. Vincent, Effect of climate change relative to ozone depletion on UV exposure in subarctic lakes, *Nature,* **404**, 484-487, 2000.

Quaite, R.E., B.M. Sutherland and J.C. Sutherland (1992) Action spectrum for DNA damage in alfalfa lowers predicted impact of ozone depletion. *Nature,* **358**, 576–578.

Ricchiazzi P., S. Yang, C. Gautier and D. Sowle, SBDART: A research and teaching software tool for plane-parallel radiative transfer in the Earth's atmosphere, *Bulletin of the American Meteorological Society,* **79**, 2101-2114, 1998.

Ruggaber A., R. Forkel and R. Dlugi, Spectral Actinic Flux and its Ratio to Spectral Irradiance by Radiation Transfer Calculations, *J. Geophys. Res.,* **98**, 1151-1162, 1993.

Ruggaber A., R. Dlugi and T. Nakajima, Modelling of Radiation Quantities and Photolysis Frequencies in the Troposphere, *J. Atmos. Chem*., **18**, 171-210, 1994

Schafer, J.S., V.K. Saxena, B.N. Wenny, W.F. Barnard and J.J. DeLuisi (1996) Observed influence of clouds on ultraviolet-B radiation. *Geophys. Res. Lett.,* **23**, 2625-2628.

Scotto, J., G. Cotton, F. Urbach, D. Berger and T. Fears (1988) Biologically effective ultraviolet radiation: surface measurements in the United States, 1974 to 1985. *Science*, **239**, 762-764.

Seckmeyer, G., B. Mayer, G. Bernhard, R. Erb, A. Albold, H. Jäger and W.R. Stockwell (1997) New maximum UV irradiance levels observed in Central Europe. *Atmospheric Environment*, **31**, 2971-2976.

Setlow, R.B. (1974) The wavelengths in sunlight effective in producing skin cancer: a theoretical analysis. *Proc. Nat. Acad. Sci. USA,* **71**, 3363-3366.

Slusser, J., J. Gibson, D. Bigelow, D. Kolinski, W. Mou, G. Koenig and A. Beaubien (1999) Comparison of column ozone retrievals by use of an UV multifilter rotating shadow-band radiometer with those from Brewer and Dobson spectrophotometers. *Appl. Opt.,* **38**, 1543-1541.

Smith, F. L. and C. Smith (1972) Numerical evaluation of Chapman's grazing incidence integral Ch(X,χ), *J. Geophys. Res.*, **77**, 3592-3597.

Taalas, P., J. Kaurola, J. Herman and N. Krotkov (2002) On the global UV changes 1980-2000, *Geophysical Research Abstracts*, **4**, Abstract #EGS02-A-06813, European Geophysical Society, XXVII General Assembly, Nice, France, 21-26 April, 2002.

Tsitas, S.R. and Y.L. Yung (1996) The effect of volcanic aerosols on ultraviolet radiation in Antarctica. *Geophys. Res. Lett.,* **23**, 157-160.

UNEP (1998) *Environmental effects of Ozone Depletion: 1998 Assessment,* United Nations Environment Programme , 205pp, 1998

Verdebout, J., A method to calculate surface UV radiation maps over Europe using GOME, Meteosat, and ancillary geophysical data, *J. Geophys. Res.,* **105**, 5049-5058, 2000.

Weatherhead, E.C., G.C. Tiao, G.C. Reinsel, J.E. Frederick, D.S. Choi and W.K. Tam. (1997) Analysis of long-term behaviour of ultraviolet radiation measured by Robertson-Berger meters at 14 sites in the United States. *J. Geophys. Res.,* **102**, 8737-9754.

Weatherhead, E.C., G.C. Tiao, G.C. Reinsel, G.C. Tiao, X.-L. Meng, D.S. Choi, W.-K. Cheang, T. Keller, J. Deluisi, D.J. Wuebbles, J.B. Kerr, A.J. Miller, S.J. Oltmans and J.E. Frederick (1998) Factors affecting the detection of trends: Statistical considerations and applications to environmental data. *J. Geophys. Res.,* **103**, 17149-17161.

Webb A.R., B.G. Gardiner, T.J. Martin, K. Leszcynski, J. Metzdorf and V.A. Mohnen (1998), Guidelines for Site Quality Control of UV Monitoring, World Meteorological Organization Global Atmosphere Watch, GAW No. 126/WMO TD No. 884, 39 p. AREP/ENV, Geneva.

Webb A.R., P. Weihs and M. Blumthaler, Spectral UV irradiance on vertical surfaces: a case study, *Photochem. Photobiol.,* **69**, 464-470, 1999.

Webb A.R., I.M. Stromberg, H. Li and L.M. Bartlett, Airborne spectral measurements of surface reflectivity at ultraviolet and visible wavelengths, *J. Geophys. Res.,* **105**, 4945-4948, 2000.

Weihs, P., A.R. Webb, S.J. Hutchinson and G.W. Middleton, Measurements of the diffuse UV sky radiance during broken cloud conditions, *J. Geophys. Res.,* **105**, 4945-4948, 2000.

Welsh, R. M. and B. A. Wielicki (1989) Reflected fluxes for broken clouds over a Lambertian surface, *J. Atmos. Sci*., **46**, 1384-1395.

Wilson, M.I., and B.M. Greenberg, 1993a. Protection of the DI photosystem II reaction center protein from degradation in ultraviolet radiation following adaptation of Brassica napus L. to growth in UV-B. *J. Photochem. and Photobiol.,* **57**, 556–563.

Wilson, M.I., and B.M. Greenberg, 1993b. Specificity and photomorphogenic nature of UV-B induced cotyledon curling in Brassica napus L., *Plant Physiol.,* **102**, 671.

WMO (1999) *WMO Scientific Assessment of Ozone Depletion: 1998,* World Meteorological Organization Global Ozone Research and Monitoring Project, Report No. 44.

Zerefos C.S., Long-term ozone and update through 2001 of UV variations at Thessaloniki, Greece, *Physics and Chemistry of the Earth,* In press.

Figure Captions

Figure 1: Map showing locations of stations making regular measurements of spectrally-resolved UV-B radiation and submitting them to the World Ozone and UV-B Data Centre (WOUDC): http://www.msc-smc.ec.gc.ca/woudc/.

Figure 2: (A) The solar spectrum above the atmosphere, from the SUSIM Atlas-1 flight (Brueckner *et al.*, 1993); (B) measured at the ground at Boulder, with Brewer #039, on June 18, 1995; and (C) June 19, 1995; (D) calculated from curve A with 297 DU of ozone and an airmass factor of 1.05, using the absorption cross sections of Molina and Molina (1986); (E) the CIE erythemal action curve.

Figure 3: UV spectra recorded at Toronto by Brewer #14, June 21, 1999. Spectral scans were made at approximately 20-minute intervals between about one-half hour after sunrise and local noon. Solar zenith angles vary between 85° and 20°.

Figure 4: Increase of UV irradiance in % for a 1% decrease of total ozone (at a total ozone amount of 300 DU) as a function of wavelength for different zenith angles. The bold continuous line shows the ozone absorption spectrum (left-hand scale). From Fioletov *et al.* (1997).

Figure 5: (a, c, e): The logarithm of the UV irradiance as a function of wavelength and time of day for May 7, 1992 (clear), May 6 (some clouds), and May 2 (occasionally heavy cloud); (b, d, f): the logarithm of the ratio of the UV irradiance to that at 324 nm as a function of wavelength and time of day for May 7, 6, and 2, 1992. Except where cloud cover is very heavy (5e, 5f), the right-hand figure is fairly flat , indicating little spectral dependence of cloud attenuation. From Fioletov and Evans (1997).

Figure 6: Climatology of surface UV-B irradiance: daily observations for a number of Canadian and other sites. For each day, the maximum UV Index value observed is shown (green dots). The red curve is an estimate of the average daily maximum clear-sky UV Index at each site for the pre-1980 period, calculated from ozone records via an empirical relationship based on UV-B and ozone values observed at Toronto for snow-free conditions (Beattie *et al.,* 1995). It clearly underestimates historical UV-B for Mauna Loa. Superimposed are the most recent complete year of observations for each site (circled points). Typical maximum values have clearly increased at most stations from the pre-1980 curve. Increases at Syowa are particularly dramatic, as this station is under the antarctic ozone hole in September-December. Note the enhancements due to snow, particularly at Resolute, Churchill, Alert, Edmonton, Saskatoon and Winnipeg.

Figure 7: Percentage change per decade in erythemal-action-spectrum-weighted UV exposure as a function of latitude, including cloud effects, estimated from combined Nimbus-7 (1979-1993) and EarthProbe (1996-1999) TOMS data. Error bars indicate 2σ uncertainties. After Herman *et al.* (1996).

Figure 8: Seasonal averages of monthly mean erythemal-action-spectrum-weighted UV exposure, including cloud effects, for Canadian latitudes, estimated from TOMS (1979-1999) data. (a) Winter (November-February) averages. (b) Summer (May-August) averages. Linear trend lines with 95% confidence limits are also shown for reference. Winter trends are about twice as large as summer trends, primarily because of the larger degree of winter ozone loss.

Figure 9: Total CIE daily irradiance for Toronto and Saskatoon from ground-based (Brewer) observations, presented as seasonal averages of monthly means. Linear trend lines with 95% confidence limits are also shown for reference. Trends are all non-significant, in large part due to the fact that total ozone has not changed as much over this period as over the previous decade.

WOUDC UV Radiation Monitoring Stations

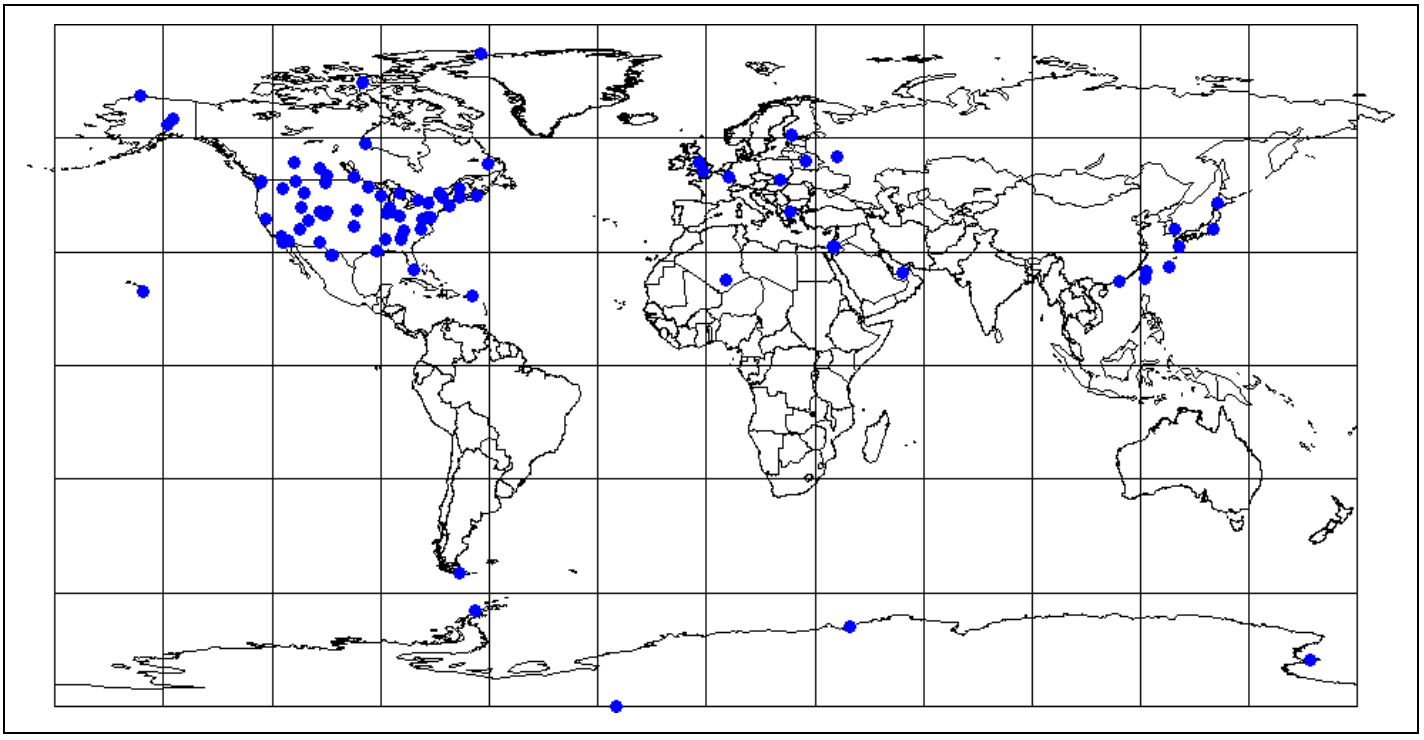

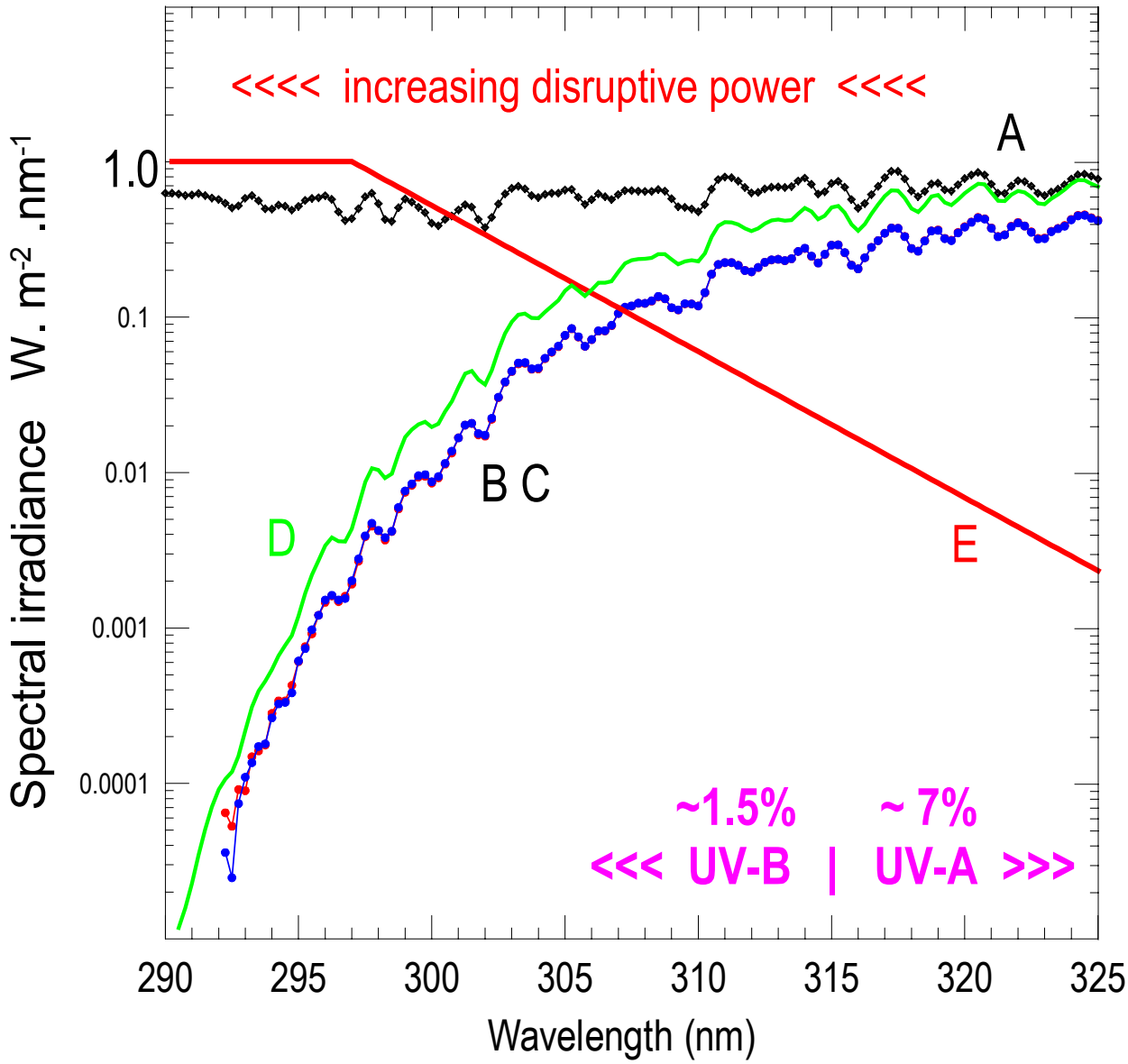
<<<< increasing disruptive power <<<<
A
B C
D
E
~1.5%
~ 7%
<<< UV-B | UV-A >>>
Spectral irradiance W. m-2 .nm-1
1.0
0.1
0.01
0.001
0.0001
290
295
300
305
310
315
320
325
Wavelength (nm)

Figure 2

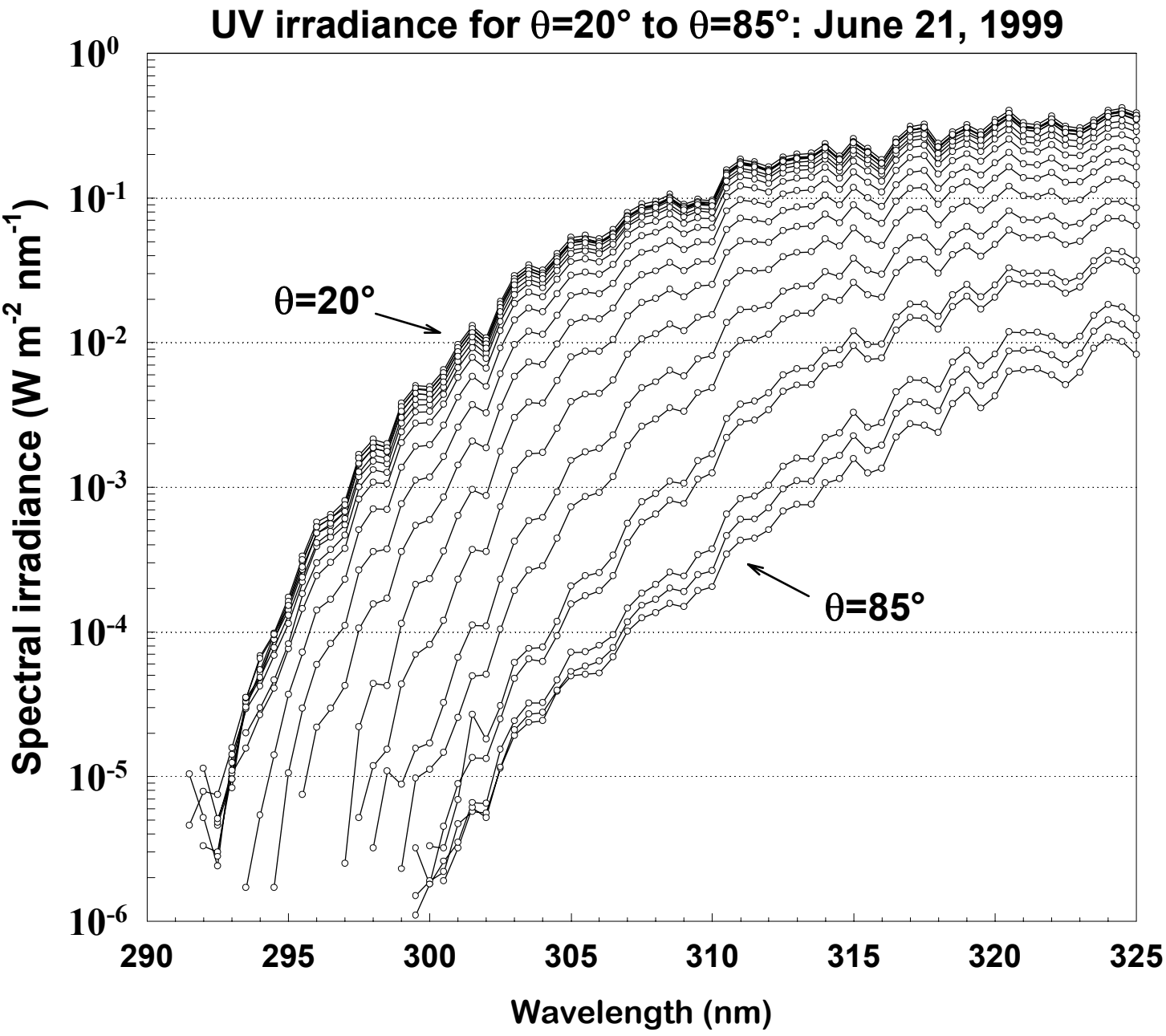
UV irradiance for θ=20° to θ=85°: June 21, 1999
Spectral irradiance (W m-2 nm-1)
10^0
10^-1
10^-2
10^-3
10^-4
10^-5
10^-6
θ=20°
θ=85°
290
295
300
305
310
315
320
325
Wavelength (nm)

Figure 3

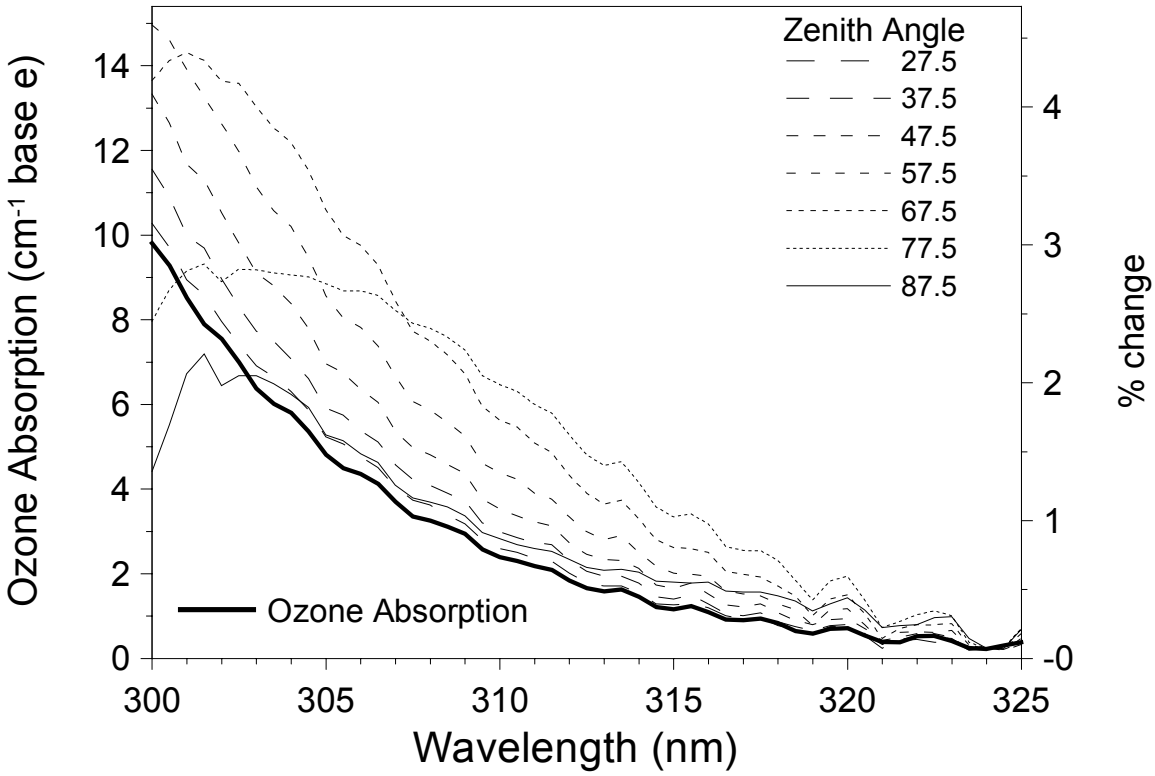
Zenith Angle
27.5
37.5
47.5
57.5
67.5
77.5
87.5
Ozone Absorption
Ozone Absorption (cm-1 base e)
% change
Wavelength (nm)
0
2
4
6
8
10
12
14
-0
1
2
3
4
300
305
310
315
320
325

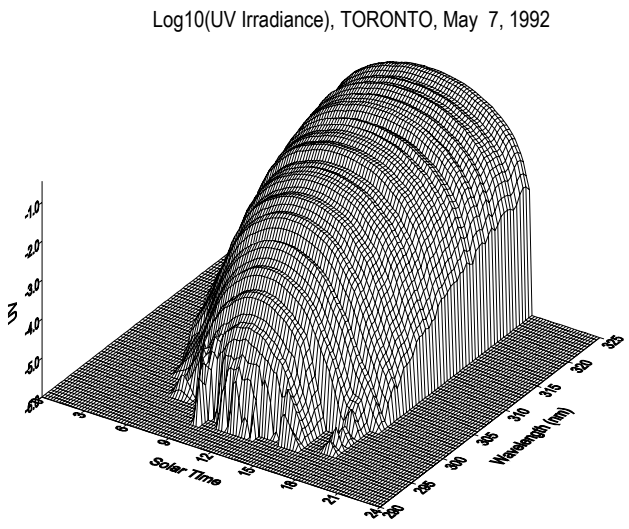
Log10(UV Irradiance), TORONTO, May 7, 1992
Solar Time
Wavelength (nm)

a

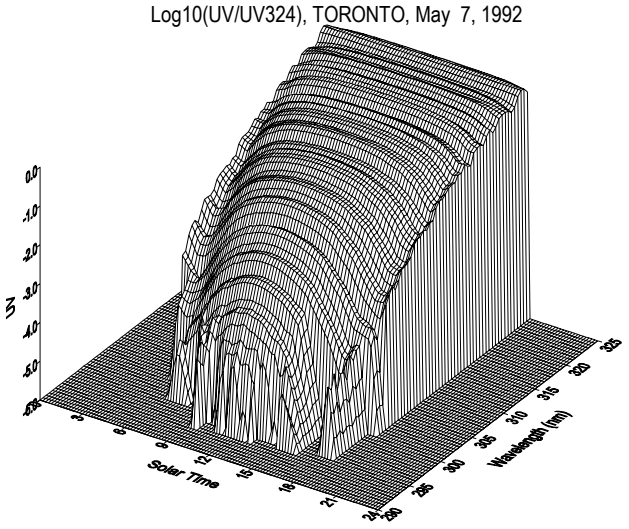
Log10(UV/UV324), TORONTO, May 7, 1992
Solar Time
Wavelength (nm)

b

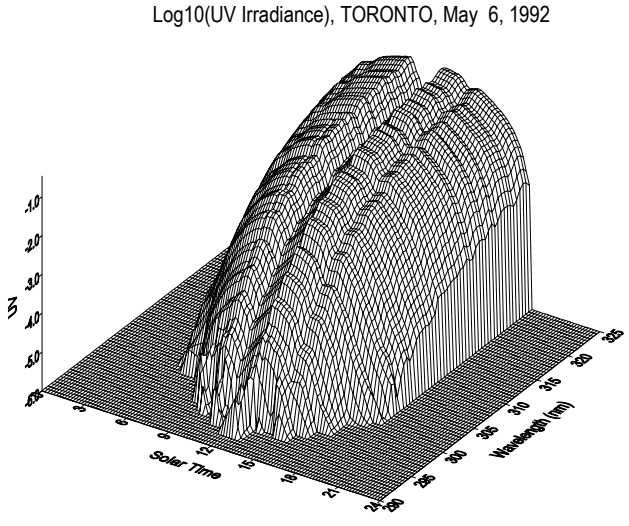
Log10(UV Irradiance), TORONTO, May 6, 1992
Solar Time
Wavelength (nm)

c

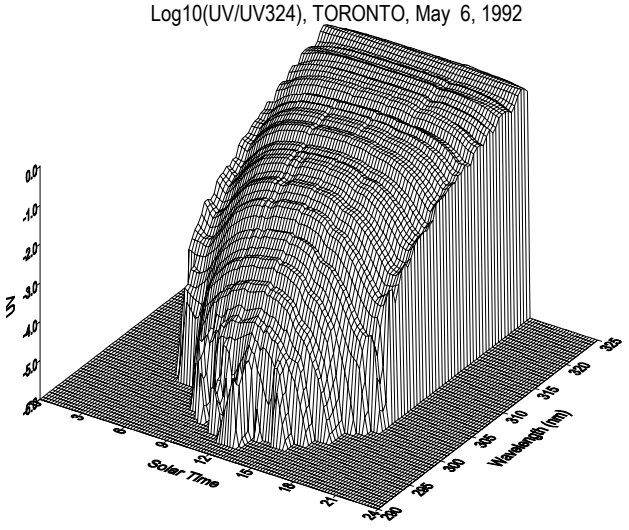
Log10(UV/UV324), TORONTO, May 6, 1992
Solar Time
Wavelength (nm)

d

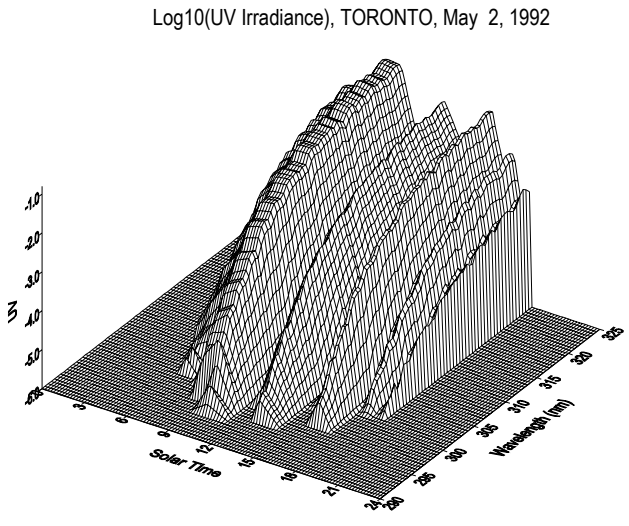
Log10(UV Irradiance), TORONTO, May 2, 1992
Solar Time
Wavelength (nm)

e

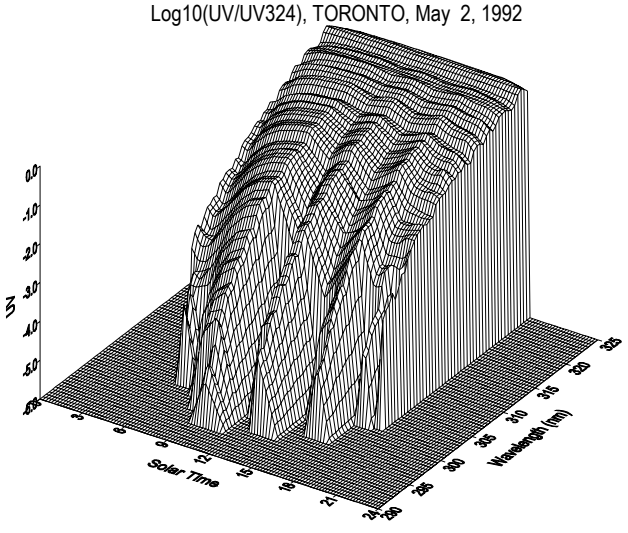
Log10(UV/UV324), TORONTO, May 2, 1992
Solar Time
Wavelength (nm)

f

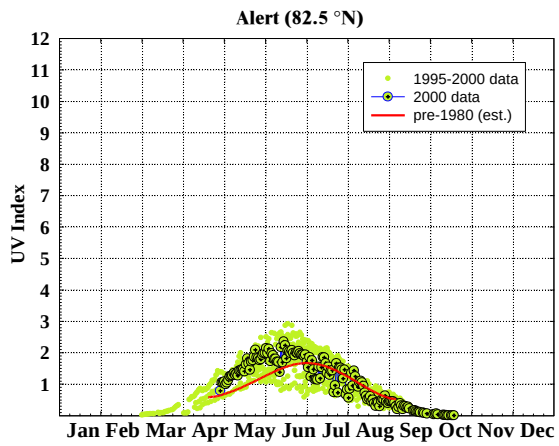
Alert (82.5 °N)
1995-2000 data
2000 data
pre-1980 (est.)
UV Index
Jan Feb Mar Apr May Jun Jul Aug Sep Oct Nov Dec

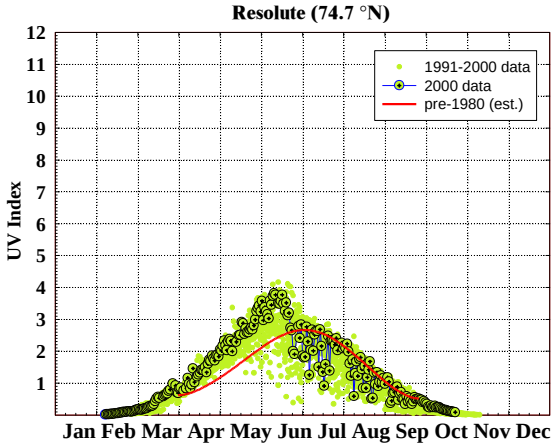
Resolute (74.7 °N)
1991-2000 data
2000 data
pre-1980 (est.)
UV Index
Jan Feb Mar Apr May Jun Jul Aug Sep Oct Nov Dec

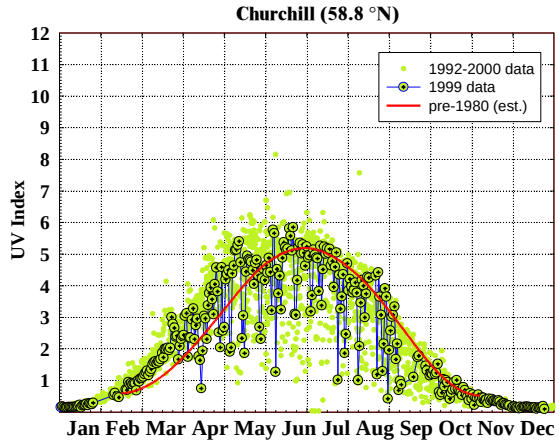
Churchill (58.8 °N)
1992-2000 data
1999 data
pre-1980 (est.)
UV Index
Jan Feb Mar Apr May Jun Jul Aug Sep Oct Nov Dec

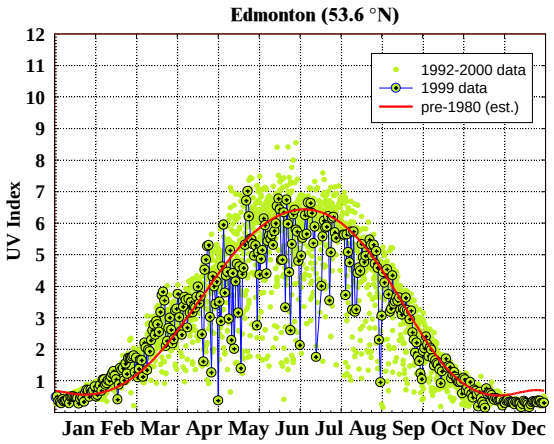
Edmonton (53.6 °N)
1992-2000 data
1999 data
pre-1980 (est.)
UV Index
Jan Feb Mar Apr May Jun Jul Aug Sep Oct Nov Dec

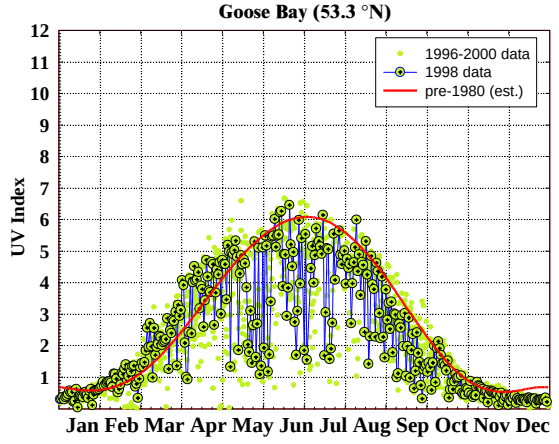
Goose Bay (53.3 °N)
1996-2000 data
1998 data
pre-1980 (est.)
UV Index
Jan Feb Mar Apr May Jun Jul Aug Sep Oct Nov Dec

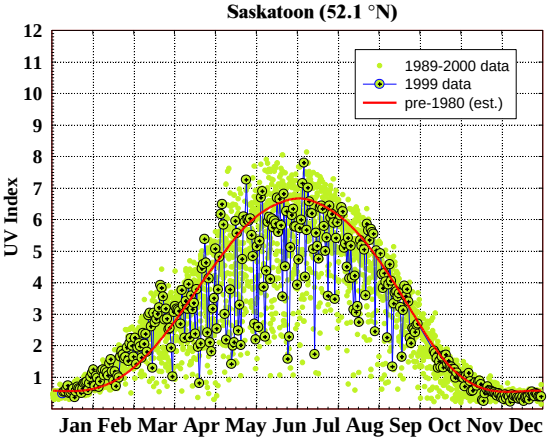
Saskatoon (52.1 °N)
1989-2000 data
1999 data
pre-1980 (est.)
UV Index
Jan Feb Mar Apr May Jun Jul Aug Sep Oct Nov Dec

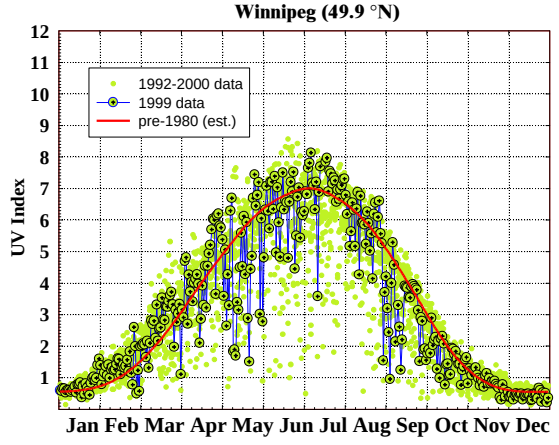
Winnipeg (49.9 °N)
1992-2000 data
1999 data
pre-1980 (est.)
UV Index
Jan Feb Mar Apr May Jun Jul Aug Sep Oct Nov Dec

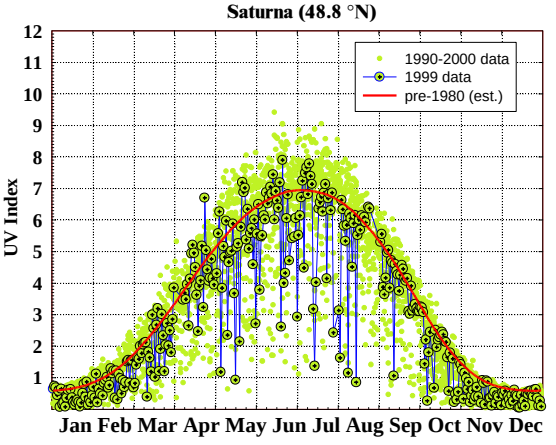
Saturna (48.8 °N)
1990-2000 data
1999 data
pre-1980 (est.)
UV Index
Jan Feb Mar Apr May Jun Jul Aug Sep Oct Nov Dec

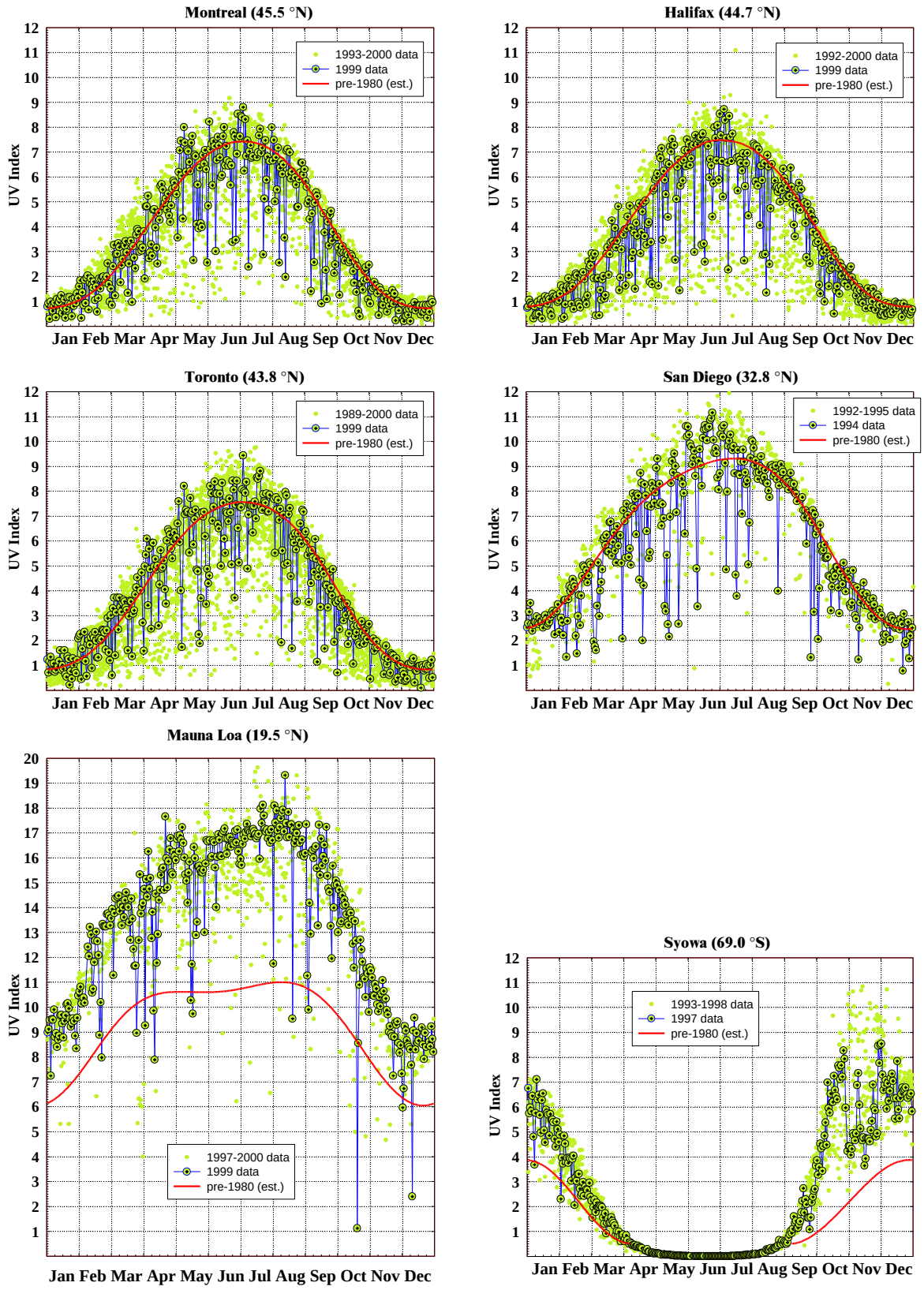
Montreal (45.5 °N)
1993-2000 data
1999 data
pre-1980 (est.)
Halifax (44.7 °N)
1992-2000 data
1999 data
pre-1980 (est.)
Toronto (43.8 °N)
1989-2000 data
1999 data
pre-1980 (est.)
San Diego (32.8 °N)
1992-1995 data
1994 data
pre-1980 (est.)
Mauna Loa (19.5 °N)
1997-2000 data
1999 data
pre-1980 (est.)
Syowa (69.0 °S)
1993-1998 data
1997 data
pre-1980 (est.)
UV Index
Jan Feb Mar Apr May Jun Jul Aug Sep Oct Nov Dec

Figure 6

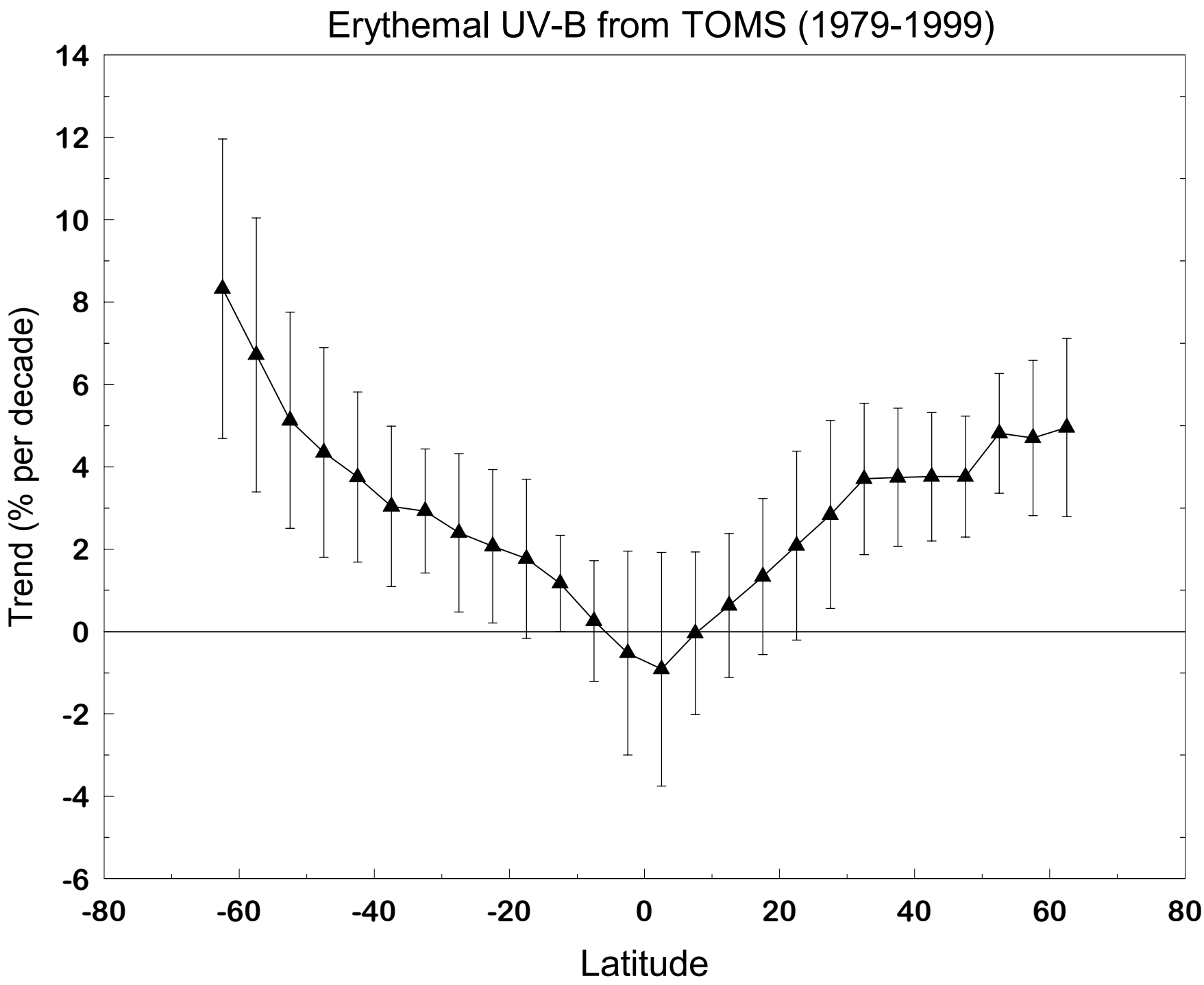
Erythemal UV-B from TOMS (1979-1999)
Trend (% per decade)
14
12
10
8
6
4
2
0
-2
-4
-6
-80
-60
-40
-20
0
20
40
60
80
Latitude

Figure 7

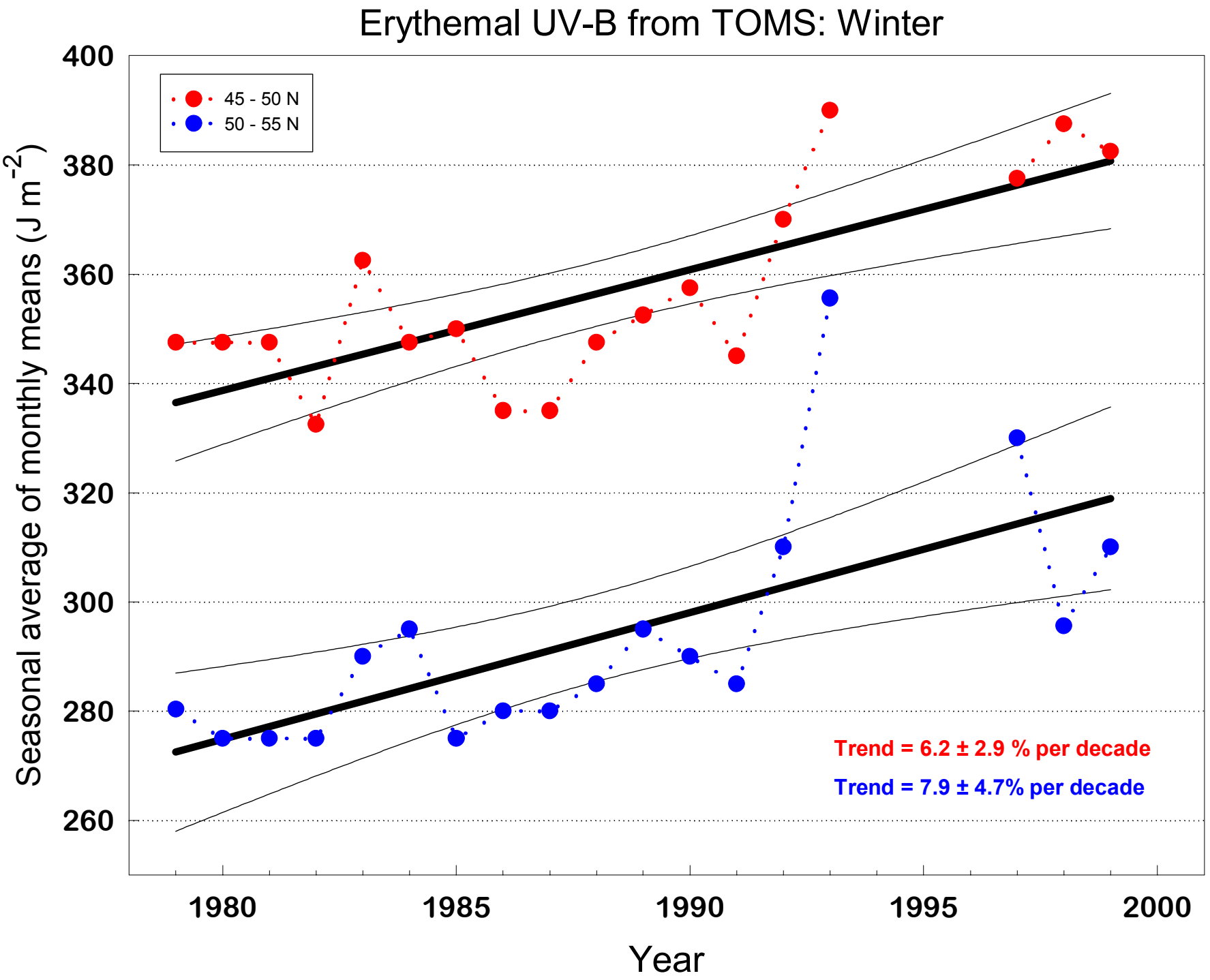
Erythemal UV-B from TOMS: Winter
45 - 50 N
50 - 55 N
Seasonal average of monthly means (J m-2)
400
380
360
340
320
300
280
260
1980
1985
1990
1995
2000
Year
Trend = 6.2 ± 2.9 % per decade
Trend = 7.9 ± 4.7% per decade

Figure 8a

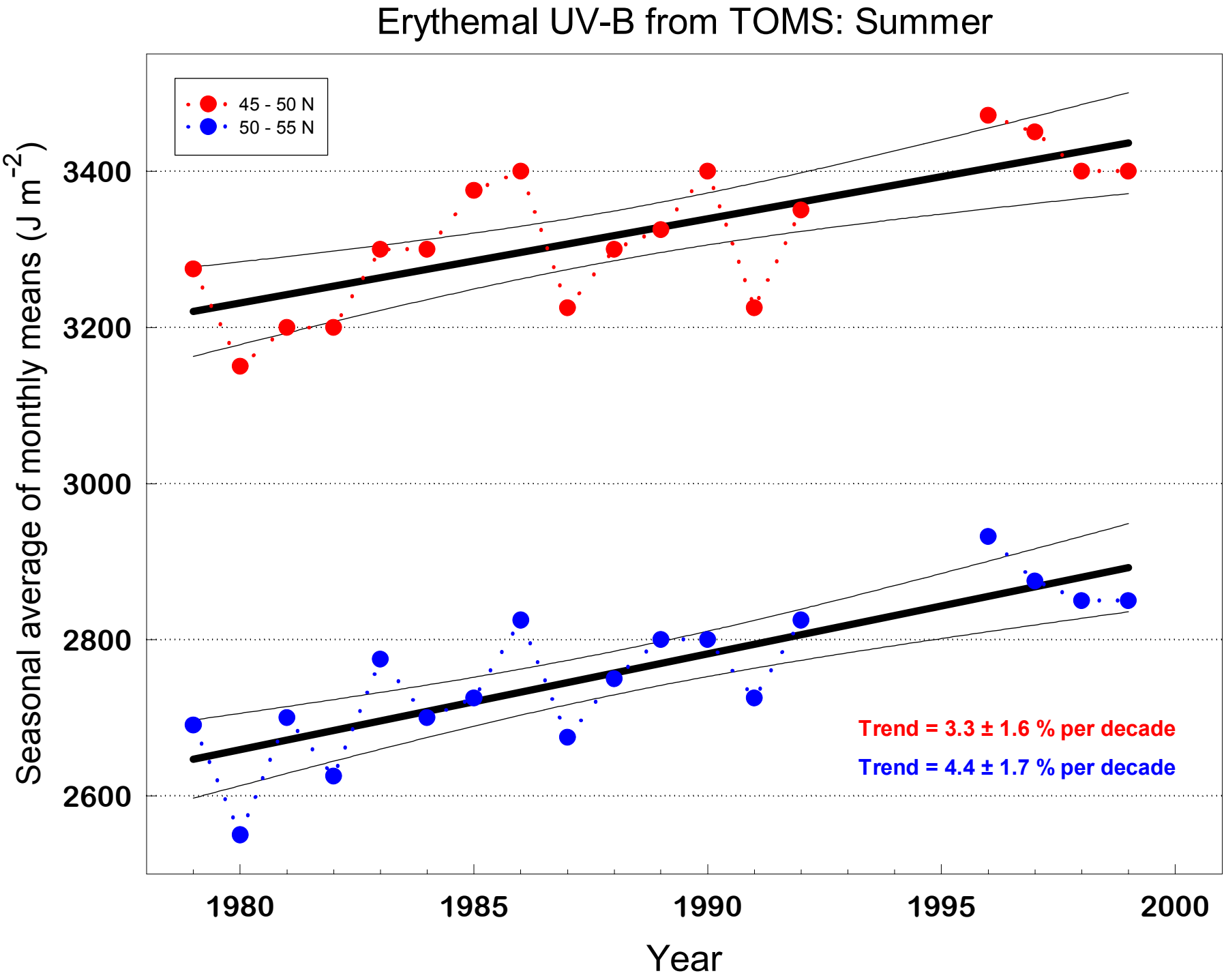
Erythemal UV-B from TOMS: Summer
45 - 50 N
50 - 55 N
Seasonal average of monthly means (J m-2)
3400
3200
3000
2800
2600
1980
1985
1990
1995
2000
Year
Trend = 3.3 ± 1.6 % per decade
Trend = 4.4 ± 1.7 % per decade

Figure 8b

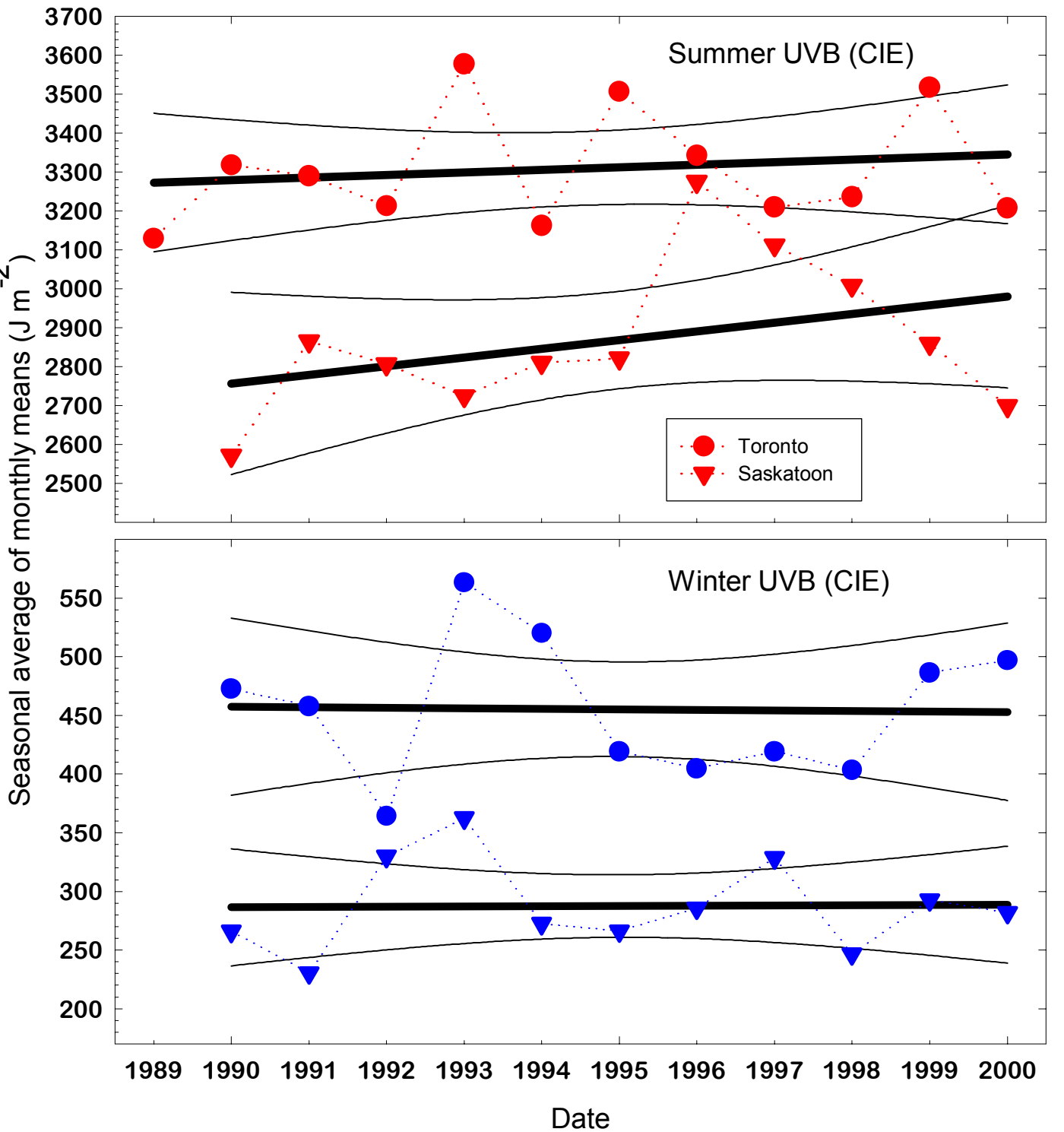
Summer UVB (CIE)
Winter UVB (CIE)
Toronto
Saskatoon
Seasonal average of monthly means (J m-2)
Date
3700
3600
3500
3400
3300
3200
3100
3000
2900
2800
2700
2600
2500
550
500
450
400
350
300
250
200
1989
1990
1991
1992
1993
1994
1995
1996
1997
1998
1999
2000

Figure 9